



THE UNIVERSITY *of* EDINBURGH

Edinburgh Research Explorer

## Mitigating air pollution strategies based on solar chimneys

**Citation for published version:**

Liu, Y, Ming, T, Peng, C, Wu, Y, Li, W, De Richter, R & Zhou, N 2021, 'Mitigating air pollution strategies based on solar chimneys', *Solar Energy*, vol. 218, pp. 11-27. <https://doi.org/10.1016/j.solener.2021.02.021>

**Digital Object Identifier (DOI):**

[10.1016/j.solener.2021.02.021](https://doi.org/10.1016/j.solener.2021.02.021)

**Link:**

[Link to publication record in Edinburgh Research Explorer](#)

**Document Version:**

Peer reviewed version

**Published In:**

Solar Energy

**General rights**

Copyright for the publications made accessible via the Edinburgh Research Explorer is retained by the author(s) and / or other copyright owners and it is a condition of accessing these publications that users recognise and abide by the legal requirements associated with these rights.

**Take down policy**

The University of Edinburgh has made every reasonable effort to ensure that Edinburgh Research Explorer content complies with UK legislation. If you believe that the public display of this file breaches copyright please contact [openaccess@ed.ac.uk](mailto:openaccess@ed.ac.uk) providing details, and we will remove access to the work immediately and investigate your claim.



# Mitigating air pollution strategies based on solar chimneys

Yang Liu<sup>1,2</sup>, Tingzhen Ming<sup>1,3, \*</sup>, Chong Peng<sup>4,5</sup>, Yongjia Wu<sup>1</sup>, Wei Li<sup>6</sup>, Renaud de Richter<sup>7</sup>, Nan Zhou<sup>5</sup>

1. School of Civil Engineering and Architecture, Wuhan University of Technology, Wuhan 430070, China

2. Department of Mechatronic Engineering, Wuhan Business University, Wuhan, China

3. School of Architectural Engineering, Huanggang Normal University, No. 146 Xingang Second Road, Huanggang 438000 China.

4. School of Architecture and Urban Planning, Huazhong University of Science and Technology, Wuhan 430074, China.

5. China Energy Group, Environmental Energy Technologies Division, Lawrence Berkeley National Laboratory, 1 Cyclotron Road, Berkeley, CA 94720 USA

6. Institute for Materials and Processes, School of Engineering, University of Edinburgh, Mayfield Road, Edinburgh EH9 3JL, UK.

7. Tour-Solaire.Fr, 8 Impasse des Papillons, F34090 Montpellier, France

## Abstract

During their rapid economic development and industrialization, megacities in the developing nations with high populations (especially in the east and south Asia) are plagued by severe air pollution problems (e.g., heavy haze), which impose a threat not only to public health but also to the sustainable development of society and the economy. To relieve the burden of air pollution for the general public, this article reviewed several geoengineering measures based on solar chimneys, which have the large-scale elimination ability on pollutants in the air, particularly for particulate matter. These geoengineering measures include driving the polluted air penetrate the planetary boundary layer into the troposphere to avoid the dramatic growth of concentrations of particulate matter, spraying water on the top of the solar chimney into the air to scavenge pollution, and intercepting fine particles in the air driven by the solar energy with large filters. Compared with traditional methods (e.g., giant spray trucks), those solar chimney geoengineering measures have the following advantages: 1) they can be operated 24 hours a day, thus keeping the pollution removal function stable and continuous; 2) they are environment-friendly and can generate clean electricity to compensate for energy consumption; 3) they are also robust and operational with very low maintenance for a long period. Given the advantages of the solar chimney geoengineering measures and the economic and human health losses caused by air pollution, those geoengineering approaches deserve to be studied further and implemented in those countries that are suffering from heavy air pollution problems.

**Keywords:** solar chimney; air pollution; haze; mitigation strategy

---

\* corresponding author, tzming@whut.edu.cn

41

42 **List of abbreviations:**

43 PBL, planetary boundary layer; PM, particulate matter.

44

45 **Main finding:**

46 Several geoengineering measures based on solar chimneys reviewed in this paper can  
47 eliminate air pollution on a large scale and generate clean electricity simultaneously.

48

49 **1. Introduction**

50 Air pollution problems caused by atmospheric aerosol are growing in megacities of  
51 many developing nations, especially for the rapidly expanding and industrializing  
52 countries with high populations (e.g., China and India). Atmospheric aerosol comprises  
53 solid or liquid particles (Hu, 2012), which can be divided by aerodynamic diameter into  
54 fine particulates (PM<sub>2.5</sub>), respirable particulates (PM<sub>10</sub>) and total suspended  
55 particulates (Hu, 2012; Liang, 2013; Pöschl, 2005), mainly from industry and transport  
56 activities, and a series of photochemical reactions (Liu et al., 2013). A high  
57 concentration of fine particles is the principal contributor to haze because the incident  
58 of sunlight is scattered and absorbed (EPA, 2020a). This is a weather phenomenon  
59 feature in reduced visibility (Wu et al., 2007), which has been observed in many  
60 countries in recent years (Gao and Ji, 2018; Jose et al., 2015; Lin et al., 2018; Sulong  
61 et al., 2017).

62 The aerosols particles in the air could alter the weather pattern. Since cloud droplets  
63 condense on tiny particles, more anthropogenic aerosols in the cloud could lead to  
64 smaller cloud droplets, more water will be retained for a longer time. As a result,  
65 precipitation would be suppressed and more solar radiation would be reflected back to  
66 space (Rosenfeld et al., 2019). The dramatic increases of aerosols in China are also  
67 believed to be the main cause of the recent southward migration of the summer  
68 monsoon rain belt resulting in the weather pattern of “South Flood-North Drought” in  
69 the summer (Li et al., 2018; Yu et al., 2016).

70 The particulate matter (PM) not only affects the environment but also imposes a  
71 threat to public health and sustainable development. Fine particles in the air can cause  
72 asthma, respiratory diseases, and even lead to death (EPA, 2020b). The adverse health  
73 effects as a result of short-term or long-term exposure to particulate matter in the air  
74 are high in many cities throughout the world (Burnett et al., 2014; Lu et al., 2016; Song  
75 et al., 2017). A special report by the Health Effects Institute showed that more than half  
76 of the global public health burden affected by the polluted air was from China and India  
77 (Institute, 2018). It was estimated that 4.2 million deaths were caused by exposure to  
78 PM<sub>2.5</sub> in 2015, with 59% of them contributed from east and south Asia (Cohen et al.,  
79 2017). Exposure to ambient fine particles was ranked as the eighth leading risk for  
80 deaths globally (Kumar, 2018).

81 A comprehensive control strategy for air pollutants is urgently needed in densely  
82 populated cities in those developing countries, which face the difficult challenge of  
83 balancing economic growth and environmental protection. To restrict air pollutant  
84 emissions, intensive remedial measures have been made by the government, including  
85 the temporary shutdown or curtail operations at industrial plants emitting large  
86 quantities of air pollutants or the traffic restrictions imposed in major metropolitan areas  
87 in China (Li et al., 2017). Although annual average concentrations of PM<sub>2.5</sub> in Chinese  
88 74 key cities decreased by 33.3%, and PM<sub>10</sub> by 27.8% between 2013 and 2017, both  
89 of the two indexes were still higher than the National Standard (35  $\mu\text{g}/\text{m}^3$ , GB 3059-  
90 2012) (Huang et al., 2018a). It was also found that the concentration of PM reduced  
91 rapidly at first, but the reduction rate slowed down gradually, which meant that long-  
92 term air quality improvement methods were needed to tackle this issue (Greenbaum,  
93 2018).

94 At the emission sources, traditional emission control devices for particles  
95 including cyclones, the electrostatic precipitators (ESP), the bag filters, and the wet  
96 scrubbers are designed for and used in specific systems in industry (e.g., coal-fired  
97 system). However, they may be effective against large particles but with unsatisfying  
98 performance against fine particles (Y.H.Pui et al., 2014). More importantly, they do not  
99 apply to the open atmosphere in public places of megacities. In China, specially  
100 designed trucks with a giant water sprayer (water cannon) are dispatched to public areas,  
101 patrolling and spraying water to the air surrounding the streets and buildings to relieve  
102 the adverse effects of PM, but which has the ability for improving air quality in a limited  
103 area.

104 To tackle the haze problems and improve urban environmental air quality, some  
105 ambitious and promising geoengineering measures have been proposed and some  
106 prototypes have been built in recent years. These measures include driving the polluted  
107 air penetrate the planetary boundary layer into the troposphere to avoid the dramatic  
108 growth of concentrations of particulate matter, spraying water on the top of the solar  
109 chimney (tower) into the air to scavenge air pollutants and intercepting fine particles in  
110 the air driven by the solar chimney with large filters (Tan et al., 2017; Yu, 2014; Zhou  
111 et al., 2015). Those geoengineering approaches newly proposed or constructed to treat  
112 aerosol were summarized in Table 1. Their scientific rationale, environmental impacts,  
113 and feasibility with some novel modifications based on the solar chimney were  
114 analyzed and compared in the following sections.

115  
116  
**Table 1**  
**Overview of Principal Air Pollution Removal Measures**

Measures	Mechanism(s) proposed
----------	-----------------------

High solar chimney	Utilizing the heat island effect to drive the polluted air up to the free troposphere (Zhou et al., 2015).
Spraying water on the top of high chimneys to wash out pollutants	Pumping water to the top of high chimneys, then spraying droplets into the atmosphere to wash out air pollutants (Lodhi, 1999; Yu, 2014; Yu, 2019).
	Scavenging the air pollutants in the spray scrubber (Cui et al., 2017).
Spraying condensed water vapor from the air to wash out pollutants	Driving the humidified air up into a high chimney to be saturated and condensed naturally (VanReken and Nenes, 2009) or with the help of a condenser (Ming et al., 2017) to create precipitation in the chimney.
	Utilizing the condensation latent heat to form self-sustained updraft air-cleaning chimneys (Bonnelle, 2004).
Air filter measures	Driving the air through a filter by the heat gained from the solar canopy (Cao et al., 2018a; Cao et al., 2018b; Cao et al., 2015; Cao et al., 2018c).
	Using an inverted U-type system to channel the filter-cleaned air back to ground level (Gong et al., 2017).

117

## 118 **2. The potential use of solar chimneys to alleviate haze**

### 119 **2.1 The solar chimney power plants**

120 The solar chimney power plant concept was initially proposed by Schlaich, and a  
 121 200 m high solar chimney power plant prototype was constructed and tested in  
 122 Manzanares, Spain (Schlaich et al., 2005). The prototype is shown in Fig. 1. It is  
 123 composed of a chimney mounted on a low circular transparent or translucent canopy  
 124 open at the periphery. As the hot air under the canopy heated by solar radiation has a  
 125 lower density than the air outside, it ascends in the chimney and generates a strong  
 126 airflow to propel the turbines installed under the chimney and produce carbon-free  
 127 renewable electricity.

128 Although the solar chimney was designed for power generation for the original  
 129 plan, many variants for other purposes based on the solar chimney have been proposed  
 130 in recent years. Using modified solar chimneys to generate freshwater from the humid  
 131 air was proposed by Wu et al. (2020). Ming et al. (2016a) suggested several measures  
 132 utilizing the solar chimney to enhance the atmospheric convection and thus to fight  
 133 global warming. Maia et al. (2019) reviewed the major studies on using the solar  
 134 chimney for desalination. Here, for the first time, the geoengineering measures for  
 135 large-scale air pollution mitigation based on the solar chimney will be reviewed in this  
 136 paper.

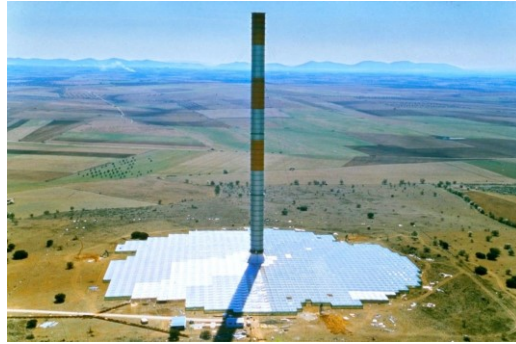


Fig. 1. Solar chimney prototype in Manzanares, Spain (Schlaich et al., 2005).

## 2.2 Proposal for the use of solar chimneys to alleviate haze

A solar chimney has been proposed to mitigate the dense haze by transferring the polluted air through the planetary boundary layer (PBL) into the high troposphere in Chinese megacities (Zhou et al., 2015). Since the PBL acts as a natural barrier to the vertical dispersion of pollutants, if the pollutants are lower than the upper edge of PBL, they spread by advection inside the PBL. While, when the pollutants travel through the boundary layer, they would extend to long distances over the troposphere (Đorđević and Šolević, 2008).

The proposed tall solar chimneys can use the urban heat island effect (the difference in air density of the warmer air in cities compared to surrounding areas) to drive air upward and transport the polluted air into the free troposphere. The urban heat island effect can be significant; the annual mean temperature difference in Beijing can be 7.78°C (Zhou et al., 2015). Those solar chimneys are able to not only break through the PBL barrier (which was shown as stable stratification in Fig. 2) but also provide a large domain for haze mixture. The PM<sub>2.5</sub> pollutants would ultimately be diluted and rendered harmless for human beings. The mechanism of this measure is illustrated in Fig. 2.

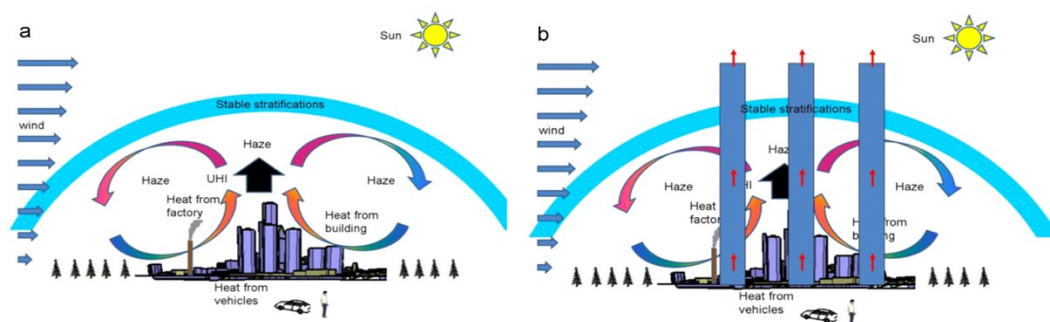


Fig. 2. (a) Haze recirculated under the PBL and (b) haze transported above the PBL by solar chimneys (Zhou et al., 2015).

Solar chimneys have several potential advantages and disadvantages. They have the potential advantage of not only removing the haze from urban residents' surroundings but also generating green energy using turbines mounted under the chimneys. Preliminary estimates also indicated that just nine solar chimneys would be enough to transfer the atmospheric air below 1 km over Beijing to a higher altitude in

164 three months of operation (Zhou et al., 2015). Disadvantages include that air pollution  
165 is not removed but transported and dispersed into higher or other areas through  
166 atmospheric motion (Huang et al., 2020b), and the following potential negative effects  
167 are difficult to predict (Tan et al., 2017). To study the rationale of this large-scale and  
168 high-efficient air pollutant removal proposal, a comprehensive analysis is made in the  
169 following part.

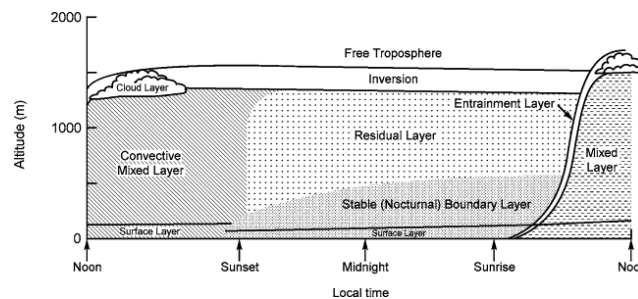
### 170 **2.3 Rationale for the use of solar chimneys to alleviate haze**

171 Since the relationships among the solar chimneys, the haze and the PBL link  
172 directly to the mitigation effects of PM in the air, this part would discuss the  
173 relationships between the PBL and the PM first, and then give the rationale for the use  
174 of solar chimneys to alleviate haze.

#### 175 **2.3.1 The planetary boundary layer**

176 The PBL is the lowest layer of the atmosphere, extending from the surface of the  
177 Earth to approximately 1000 m. The exchange rate of particulate matter (PM) between  
178 the air below and the free troposphere above the boundary layer is affected by the  
179 turbulent airflow in this layer (Brancher et al., 2017).

180 The internal structure of PBL varies significantly with the time of day. When the  
181 sun rises, a relatively higher convective mixed layer is generated due to the heat gain  
182 from the sun radiation, where the air pollutants spread and mix within it by turbulent  
183 airflow. When the sun falls, a relatively lower stable boundary layer is formed because  
184 of the decayed turbulent airflow, with the residual layer left in the upper part (Hu, 2015).  
185 See Fig. 3.



186  
187 Fig. 3. Schematic of the daily mix process within PBL (Finlayson-Pitts and Pitts, 2000).

#### 188 **2.3.2 Relationship between the PBL and the haze**

189 The relationship between the haze and the PBL is reciprocal, as heavy aerosols  
190 pollution could affect the height and structure of PBL (Liu et al., 2019; Miao et al.,  
191 2018; Quan et al., 2013; Zhong et al., 2019b). When haze occurs, the radiation is  
192 absorbed by aerosols or scattered away, which reduces incoming solar radiation on the  
193 Earth's surface, leading to smaller surface heat gain and weaker turbulence (Li et al.,  
194 2020). In a case study, the radiative cooling effects of aerosols would cause a reduction  
195 of 89% surface direct radiation exposure accumulated in one day during a haze event  
196 (Zhong et al., 2018). This cooling effect would result in a contraction of PBL due to the  
197 weaker turbulence. On another side, the solar energy absorbed by the aerosols would  
198 heat the upper PBL, making a temperature inversion within the PBL (Ding et al., 2016;

199 Huang et al., 2018b; Zhong et al., 2018). This inversion would be adverse for the  
200 transportation of pollution from the lower surface layer (which is colder) to the higher  
201 atmosphere (which is warmer).

202 The lowered PBL caused by the aerosol radiation cooling effects compresses the  
203 aerosol and leads to an increase in aerosol concentration, making the haze more serious.  
204 This positive feedback loop can lead to a continuous increase in aerosol concentration  
205 (Quan et al., 2013). The way in which accumulated aerosol pollution would alter the  
206 height and structure of PBL due to the radiative cooling and this contracted and stable  
207 PBL would further promote aerosol accumulation was called "two-way feedback  
208 mechanism" (Liu et al., 2019; Zhong et al., 2019b).

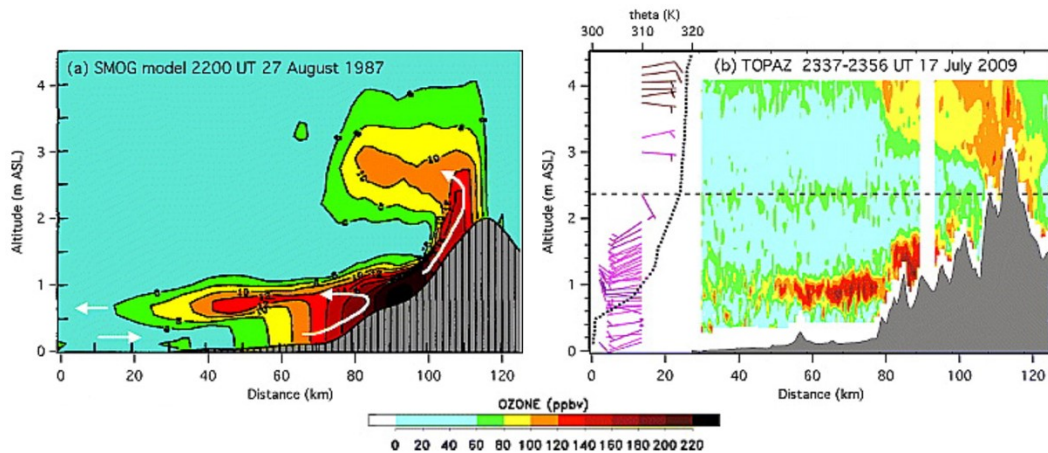
209 It was also found this positive feedback would trigger the dramatic growth of fine  
210 particulate matter (a tenfold or more increase from tens  $\mu\text{g}/\text{m}^3$  in 2-3h), leading to a  
211 persistent haze event. The dramatic growth of fine particulate matter was regarded as  
212 the first and most important stage in the four evolution stages of the severe haze episode  
213 (Sun et al., 2016a). The lower and stable planetary boundary layer was attributed to  
214 being the prime reason (approximately 84% of the contributory causes) for the dramatic  
215 growth of PM<sub>2.5</sub> in the initial cumulative phase of a persistent haze event (Zhong et al.,  
216 2017). The threshold value for the dramatic growth of PM<sub>2.5</sub> was proved and suggested  
217 as  $100 \mu\text{g}/\text{m}^3$ , under which the dramatic growth of PM<sub>2.5</sub> and the occurrence of a  
218 persistent haze event would be avoided (Zhong et al., 2019a). A similar PM threshold  
219 for a non-linearly quick improvement of air quality from the haze event (the contrary  
220 process to the haze formation) was also suggested (Ding et al., 2016).

221 The two-way feedback mechanism shows that the concentration of accumulated  
222 particle pollutants should be restricted within a certain level (threshold) by any methods  
223 (e.g., the solar chimney measure). When the concentration reaches the specific level  
224 (threshold), the height and structure of the boundary layer would be changed due to the  
225 radiative cooling, which would significantly worsen the pollution diffusion condition  
226 or even close the way for it (Zhong et al., 2019b), leading to the dramatic growth of  
227 particulate matter.

### 228 **2.3.3 Natural chimney effects on pollution dispersion**

229 The measure of solar chimneys to disperse air pollution takes advantage of the  
230 chimney effect that is also found in cities located near high mountains. This effect  
231 similarly does a certain amount of pollution dispersal naturally which is called the  
232 "mountain chimney effect" (Rong and Turco, 1996). The vertical transportation of  
233 ozone over the Los Angeles Basin was simulated and shown in Fig. 4a. Ozone measured  
234 above this Basin in 2009 (Fig. 4b) also showed ozone was transferred from the surface  
235 of the Earth to the troposphere due to the lift force of the San Gabriel Mountains  
236 (Langford et al., 2010).





237  
 238 Fig. 4. Cross-section of ozone concentration (parts-per-billion-by-volume, ppbv) over the LA  
 239 Basin, (a) in 1987, and (b) in 2009 (Langford et al., 2010).

240 The mountain chimney effect (also called the mountain-valley breeze) was  
 241 observed using aircraft measurements (Chen et al., 2009). The authors observed a  
 242 distinct two-pollution-layer structure in the region of Beijing, one near the ground  
 243 within the PBL and another elevated layer above the free troposphere at an altitude of  
 244 2500 to 3500 m with identical in composition and similar concentrations. This  
 245 mountain chimney effect could lead to a reduction of PM<sub>2.5</sub> by 70-80  $\mu\text{g}/\text{m}^3$  and the  
 246 achievement of “APEC Blue” (blue sky days during APEC summit in Beijing) (Sun et  
 247 al., 2016b). It was also observed that the concentrations of PM started to build up  
 248 immediately when the mountain chimney effect disappeared.

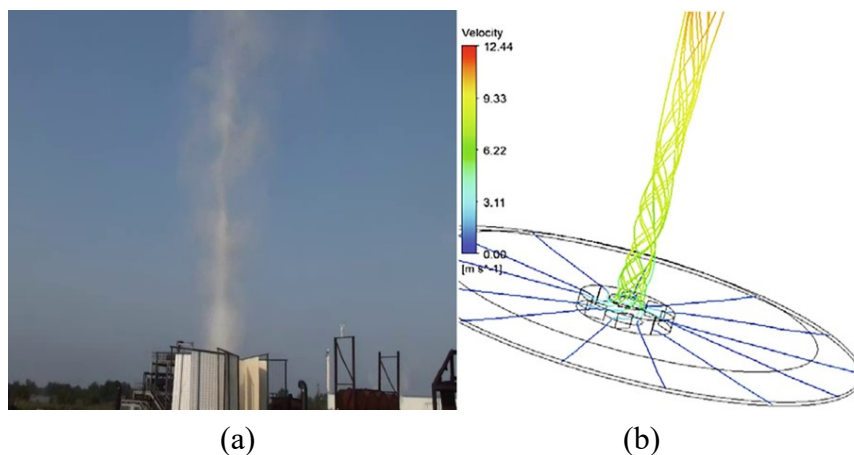
249 The evidence discussed above shows that the solar chimneys can be a feasible way  
 250 to drive pollutants across the PBL and vertically transport them to the troposphere by  
 251 taking advantage of the chimney effect in those megacities plagued by the haze events.  
 252 Although the solar chimneys cannot physically eliminate pollution and can only  
 253 transport air pollutants in the PBL into the free troposphere, it provides an opportunity  
 254 to keep the concentration of pollutants within a controllable level, otherwise, the air  
 255 quality would deteriorate because of the “two-way feedback mechanism”. In particular,  
 256 the solar chimneys can keep fine particles under the specific concentration threshold to  
 257 avoid the dramatic growth of fine particulate matter that could facilitate the initiation  
 258 of persistent haze events.

#### 259 **2.4 Evaluation of the high solar chimney measure**

260 First, a high chimney is needed in this measure. The variations of height of the  
 261 PBL above Wuhan were studied, which showed that the height of the PBL displayed  
 262 clear seasonal variations (Zhu et al., 2018). In the daytime, the year-mean height of  
 263 PBL varied around 1100 m (higher in summer and lower in winter), and the mean height  
 264 during winter varied from 903 m to 1044m. In the nighttime, the year-mean height of  
 265 PBL was never higher than 659 m. As the haze happened more frequently in the winter  
 266 than summer (Zheng et al., 2019) and the airflow still had upward vertical velocity at  
 267 the outlet of the chimney, a solar chimney of 1000 m would be sufficient in this location.

268 Second, the high cost of the chimney must be considered in this measure. Floating  
269 solar chimneys, which utilized the buoyancy forces of the balloon attached to the  
270 chimney to sustain the weight of the structure, have been proposed and studied to solve  
271 the problems of high-cost solar chimney structures (Papageorgiou, 2007; Papageorgiou,  
272 2008). A floating solar chimney that is stiffened by attachment to a mountainside has  
273 also been proposed, able to extend several thousand meters up a high mountain (Zhou  
274 and Yang, 2009). Floating chimneys are less expensive than those made of reinforced  
275 concrete with a similar dimension compared using the full life-cycle cash flows analysis  
276 (Zhou et al., 2009b).

277 Third, the construction of the high chimney may be an engineering problem even  
278 though the floating chimneys are used. A concept of atmospheric vortex engine was  
279 proposed to generate a cyclone column by Louis Michaud to replace high chimney with  
280 the cyclone (<http://vortexengine.ca>, accessed on 12 October 2020). The air heated by  
281 the canopy (or other waste heat) travels through the swirl vanes set at the center of the  
282 canopy. The hot air rises from the canopy with rotation; thus, a cyclone is formed. The  
283 cyclone could suck the out air into the device due to the negative pressure produced by  
284 the centrifugal force and the density (temperature) difference. Because of the high  
285 tangential velocity of the cyclone, the heat exchange between the cyclone and the cold  
286 ambient air was isolated. The cyclone will continuously rise until the vortex is weak  
287 and the airflow temperature reaches the same as the surrounding air. A prototype was  
288 built by Michaud's team (see Fig. 5a) and simulated by Zuo et al. (2020) (see Fig. 5b).  
289 In this simulation, with 8 m high swirl vanes and a 112 m-radius collector, the cyclone  
290 can rise more than 200 m. This technology may meet the engineering challenge of the  
291 construction of a high chimney in the future.



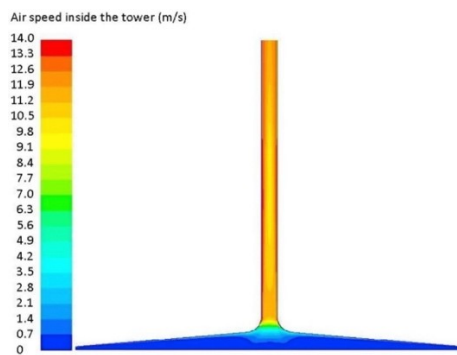
294 Fig. 5. The atmospheric vortex engine, (a) The prototype (<http://vortexengine.ca>), and (b) its  
295 simulation result (Zuo et al., 2020).

296 Fourth, when the urban heat island is formed, the air temperature in the urban area  
297 is larger than in the rural area. The temperature difference is compared between two  
298 places with a long distance between them. A chimney just erected in the downtown of  
299 the city will not induce the natural flow inside due to the small temperature difference

300 between inside and outside. A high chimney with a canopy to gather heat energy from  
301 the sun is needed in this measure.

302 Fifth, to ultimately settle the problem of PM, a similar 1 km filter-contained solar  
303 chimney has been proposed to filter the air pollution driven by the urban heat island  
304 effect and to compensate for the replacement expense of filters by the generated  
305 electricity from the turbines (Tan et al., 2017). It was claimed that the achievable health  
306 benefits (lower premature mortality and reductions in hospital admissions for  
307 respiratory issues) gave this filter-contained solar chimney a positive return on  
308 investment.

309 Lastly, one may concern that a high wind speed under the canopy will influence  
310 the daily life of citizens nearby. The velocity of air in the solar chimney was illustrated  
311 by Fig. 6 in a case study under the weather conditions in Orkney, Scotland (Jafarifar et  
312 al., 2019). The total height of this system is 202 m, the canopy radius is 120 m, the  
313 canopy inlet height is 2 m, and the radius of the chimney is 5m. It was shown that the  
314 velocity of the air under the canopy is much lower than in the chimney because the  
315 radius of the canopy is several times larger than the radius of the chimney.



316  
317 Fig. 6. The velocity of air inside the solar chimney (Jafarifar et al., 2019).  
318

### 319 **3. Elimination of air pollution by spraying water droplets in solar chimney**

320 A solar chimney can transport air pollutants into the free troposphere and provide  
321 an opportunity to keep the concentration of pollutants within a controllable level, but it  
322 cannot physically eliminate the pollution.

323 Many researchers have studied the effect of eliminating pollutions by water  
324 droplets passing through the air. The geoengineering approach by the means of spraying  
325 water droplets on high chimneys to eliminate air pollution, which mimics the rain  
326 process, is reviewed in this section.

#### 327 **3.1 The mechanism of fine aerosol removal by water spraying**

328 When a water droplet passes through the haze, the aerosol in the air would be  
329 scavenged by the droplet and gathered, thus cleansing the air. The scavenging  
330 mechanisms at work are direct inertial impaction, Brownian diffusion, diffusiophoresis  
331 (vapor concentration gradient), thermophoresis (temperature gradient), and deposition  
332 because of various electrical interactions (Cherrier et al., 2017; Wang et al., 2010).

333 Brownian diffusion and electrical interactions dominate the ultrafine aerosols  
334 scavenging process (radius  $r < 0.01 \mu\text{m}$ ), while coarse-mode or larger aerosols with  
335 radius  $r > 1 \mu\text{m}$  are collected as a result of inertial impaction and interception (Chate  
336 et al., 2011; Seinfeld et al., 2006).

337 Fredericks and Saylor (2016) gave a refined model to predict the droplets  
338 scavenging via inertial impaction for a relatively large particle. The diffusional  
339 collection efficiency of submicron particles by a raindrop (Kang et al., 2015). For  
340 particles around the Greenfield gap (Greenfield, 1956), microphysical modeling was  
341 proposed to estimate the scavenging efficiency, where particles are significantly  
342 sensitive to inertia and Brownian motion (Cherrier et al., 2017). Wang et al. (2010)  
343 gave the contour lines of the total droplet-particle scavenging efficiency as a function  
344 of both droplet diameter and particle diameter. Based on this relationship, a two-stage  
345 spray system was devised to promote scavenging efficiency. An air-atomized nozzle  
346 was placed at the first stage for the sub-micron particle collection through diffusion by  
347 the generated droplets around  $1 \mu\text{m}$ . Then, a full cone nozzle would jet water droplets  
348 around  $20 \mu\text{m}$  to collect those droplets at the first stage by the interception and inertial  
349 impaction effect (Koo et al., 2010).

350 The aerosol scavenging effects of the rain droplets were also observed by many  
351 researchers (Lu et al., 2019; Roy et al., 2019; Yoo et al., 2014) when the rain droplets  
352 pass through the polluted air. It was claimed the rain can clean up 40% of the PM<sub>2.5</sub> in  
353 the study area due to the scavenging effect (Lu et al., 2019). It was observed that the  
354 fine particles with a diameter between  $0.2$  and  $0.4 \mu\text{m}$  were mainly scavenged by rain  
355 droplets with a diameter ranging from  $0.3$  to  $1 \text{mm}$ , while the coarse particles ( $>1 \mu\text{m}$ )  
356 could be efficiently collected by all drop sizes, mostly from raindrops larger than  $1.5$   
357 mm (Blanco-Alegre et al., 2018). A geoengineering approach by the means of spraying  
358 water into the polluted air on the top of high buildings on the scale of a whole city,  
359 which aimed to mimic the rainfall, was proposed to scavenge the aerosols in the air (Yu,  
360 2014). It was also claimed that the enhanced ambient moisture through spraying would  
361 moderate ozone pollution at ground level by the prevention of ozone formation and the  
362 destruction of the ozone photochemical reaction chain (Yu, 2019).

### 363 **3.2 Synergies of solar chimneys coupled with water spraying**

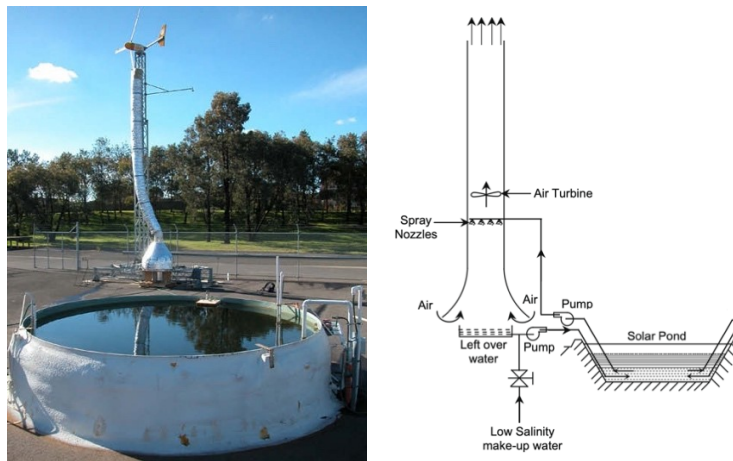
364 The geoengineering approach by spraying water into the polluted air on the top of  
365 high buildings is creative and it can keep the air around the buildings with special duties  
366 (e.g., the hospitals) clean. But to remove the air pollutants on the city scale, a more  
367 efficient method should be proposed, since the polluted air needs to be drawn to the  
368 area that is spraying. This creative geoengineering approach could be improved by  
369 spraying water droplets within a solar chimney.

370 Spraying water on the top of the solar chimney to suppress air pollution in big  
371 cities was proposed and gave the advantages compared with the rain scavenging process  
372 (Lodhi, 1999). Those advantages include: 1) the spray nozzle could be selected for the

373 particulate matter with specific diameters; 2) a continuous spraying system that can  
374 work for 24 hours a day; 3) a controllable rate of airflow driven by the air pressure  
375 difference.

376 Spraying water into the solar chimney involves not only the aerosol scavenging  
377 process but also heat and mass exchanges between the droplets and air during direct  
378 contact. If the sprayed water droplets are hotter than the air (e.g., in the cold winter),  
379 the heat is transferred from water to air. Cold air enters from the bottom of the solar  
380 chimney and becomes saturated and warmer as a result of the sensible and latent heat  
381 transferred from water. Both the temperature and humidity increase reduce the air  
382 density and produce the updraft airflow in the chimney (Akbarzadeh et al., 2009; He et  
383 al., 2016). If the sprayed water droplets are colder than the air (e.g., in summer), heat  
384 is transferred from the air to water droplets, which results in a decline in the air  
385 temperature. The decreased air temperature increases the air density and induces the  
386 natural downdraft flow in the chimney.

387 The concept of spraying hot brine in the solar chimney (see Fig. 7) was proposed  
388 by Akbarzadeh et al. (2009). The brine in a solar pond (60,000 m<sup>2</sup>) heated by the solar  
389 radiation was sprayed in the chimney to warm the air and form the natural updraft flow  
390 in the chimney. Air velocity could reach 17.1m/s (which means  $4.83 \times 10^6$  m<sup>3</sup>/h air will  
391 be purified) in a 200m high chimney with a diameter of 10 m when the air was heated  
392 from 20°C and 50% relative humidity to 60°C and 100% relative humidity. During this  
393 process, the water loss due to evaporation was about 165.8 kg/s. For comparison,  
394 441kg/s water will be lost in a typical cooling tower to reject condenser heat from a 500  
395 MW power plant (Leffler et al., 2012).

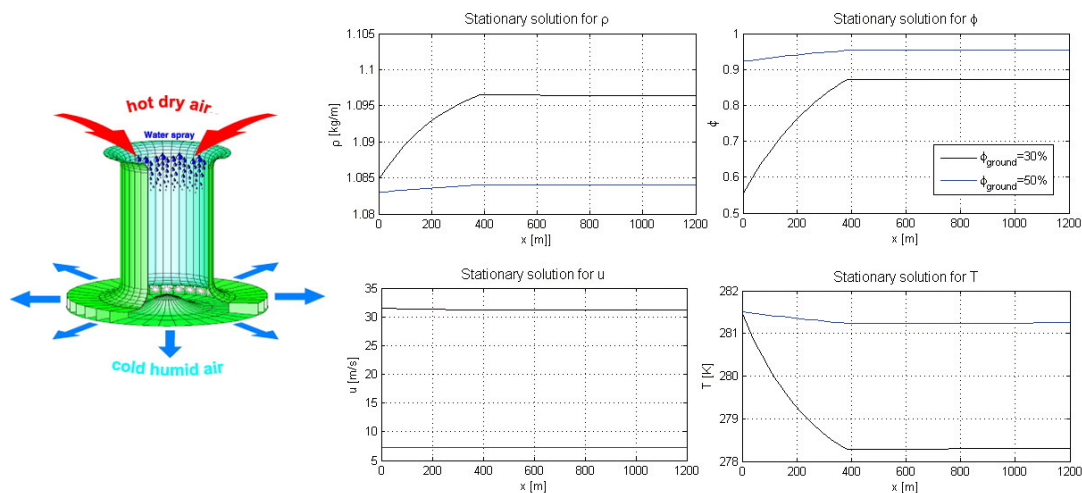


396  
397 Fig. 7. The picture of a solar chimney combined with a solar pond and its schematic design  
398 (Akbarzadeh et al., 2009).

399 Spraying cooler water in the solar chimney to generate downdraft flow was called  
400 Energy Tower (Altmann et al., 2005). By cooling hot and dry air through the  
401 evaporation of water spray, the air velocity at the bottom of the 1200 m high tower with  
402 a diameter of 400 m could reach 17.8 m/s, while the sprayed water discharge was 14.2  
403 m<sup>3</sup>/s. For the purpose of treatment of air, such a high tower is not needed and the high

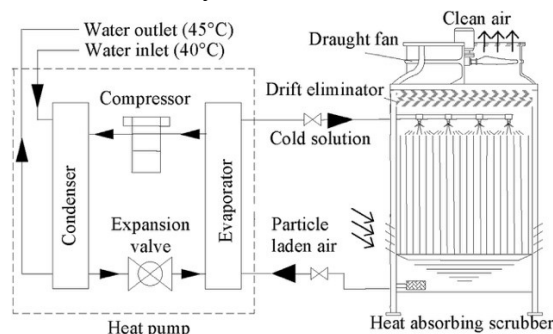


404 speed of airflow may disturb the residents near around. Variations of the main  
 405 parameters of air (density  $\rho$ , relative humidity  $\phi$ , air velocity  $u$ , and the temperature  
 406 of air  $T$ ) in this 1200 m high tower against the distance from the top ( $x$ , m) are presented  
 407 in Fig. 8 (Bauer and Gasser, 2012). From this figure, both the temperature and the  
 408 relative humidity of the air will get the final value after it travels 400 m down from the  
 409 top. So, the need for such a high tower should be discussed when it is converted to treat  
 410 pollution in the air. When the relative humidity of ambient air  $\phi$  is 50%, the final  
 411 velocity of air is about 7 m/s. The final velocity is about 32 m/s when  $\phi$  is 30%.



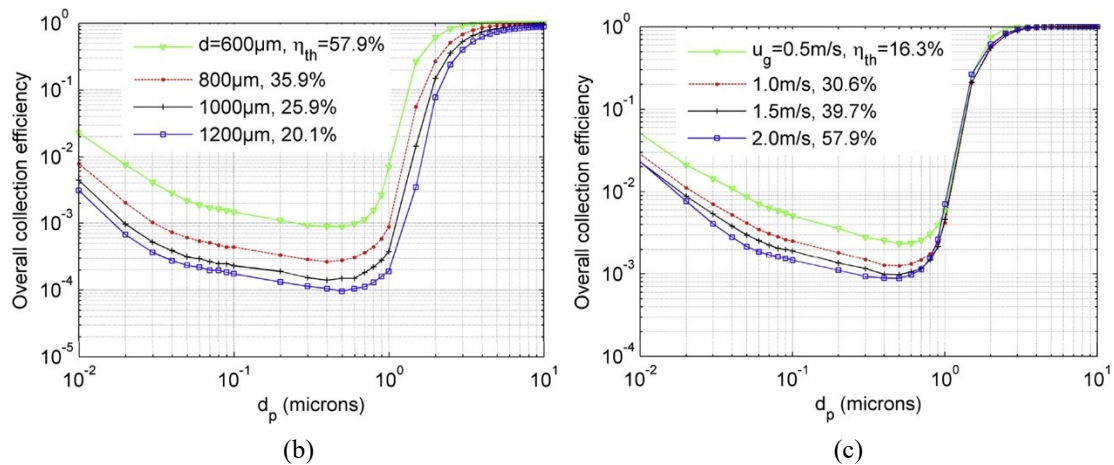
412  
 413 Fig. 8. Variations of the parameters of air in the tower against the distance from the top ( $x$ ,  
 414 m), the blue line is  $\phi=50\%$ , the black line is  $\phi=30\%$  (Bauer and Gasser, 2012)

415 A heat-absorbing scrubber was proposed to mitigate haze pollution and absorb  
 416 heat from the air (Cui et al., 2017). The cold water from the evaporator is sprayed on  
 417 top of the scrubber, absorbing heat from the warm air, then transfers the heat to the heat  
 418 pump system to supply warm water in a building. During the direct contact between the  
 419 water droplets and the air, the pollutants in the air are scavenged by the water droplets.  
 420 The scavenging efficiency (which is defined as the ratio of the particle concentration  
 421 reduced to the inlet particle concentration) depends on the diameter of the particle ( $d_p$ ,  
 422 microns), the diameter of water droplets ( $d$ ,  $\mu\text{m}$ ) and the relative velocity ( $u_g$ , m/s). See  
 423 Fig. 9b and Fig. 9c. The  $\eta_{th}$  is heat transfer efficiency. Smaller water droplets and a  
 424 lower relative velocity between droplets and air are preferred for the scavenge of  
 425 particles, but a higher relative velocity will transfer the heat faster and suck in more air.



426  
 427

(a)



428  
429  
430  
431  
432  
433  
434  
435

Fig. 9. The heat-absorbing scrubber, (a) schematic diagram, (b) collection efficiency varies with droplets diameter, and (c) collection efficiency varies with air velocity (Cui et al., 2017).

The devices involving aerosol scavenging process or simultaneous water-air heat and mass transfer process are summarized and reviewed in Table 2. Although those devices do not have the large-scale scavenging ability as the solar chimney geoengineering approach, they provide the basic principles for the study on this method.

**Table 2**  
**Comparison between Some Similar Devices with the Solar Chimney Measure**

Devices	Initial design objectives	Differences
Heat absorbing scrubber	To acquire heat from the air and scrub the air by water spray (Cui et al., 2017).	<ol style="list-style-type: none"> <li>1. Limited distance for droplets and air direct contact due to the tower height.</li> <li>2. Air is driven into the tower by the fan, not by the air pressure difference.</li> <li>3. No power generation to offset the pump and fan consumption.</li> </ol>
Natural draft wet cooling tower	To cool the cycling water of steam turbines in the power plant (Wei et al., 2020).	<ol style="list-style-type: none"> <li>1. The scavenging effect of sprayed water was not considered.</li> <li>2. Limited rain zone height for droplets-air contact to save pump energy (Zhao et al., 2016).</li> <li>3. No power generation to offset pump consumption.</li> </ol>
Spray passive downdraft evaporative cooling system	To clean and cool the captured air using water evaporation for space cooling in the building (Kang and Strand, 2018).	<ol style="list-style-type: none"> <li>1. Limited distance for droplets and air direct contact due to the tower height.</li> <li>2. No power generation to offset pump consumption.</li> <li>3. The air volume is determined by both the air pressure difference and the wind catcher.</li> </ol>
Energy tower	To produce energy by spraying salt water in the hot and dry climate (Omer et al., 2008b).	<ol style="list-style-type: none"> <li>1. The scavenging effect of sprayed water was not considered.</li> <li>2. Complete evaporation of the falling water droplets to maximize the energy generation from the tower (Omer et al., 2008a), while the complete evaporation must be avoided in a solar chimney as droplets are needed to carry the particles down to the ground.</li> </ol>

436  
437

To summarize, it is demonstrated that the water spray system can scavenge the

438 pollution in the air, although the scavenging efficiency depends on the spray nozzle  
439 type, spray pattern, water mass flow rate, spray angle, and droplet size (Sun et al., 2017).  
440 One may concern that the pollution in the air will be transferred to the water and  
441 contaminate the water. However, this water collected after the spraying process is quite  
442 different from the industrial wastewater, which has the same property as the natural  
443 rainwater (the air pollution will also be gathered by the rainfall). The water collected  
444 after spraying can be treated as rainwater at a small cost (compared with industrial  
445 wastewater or domestic sewage).

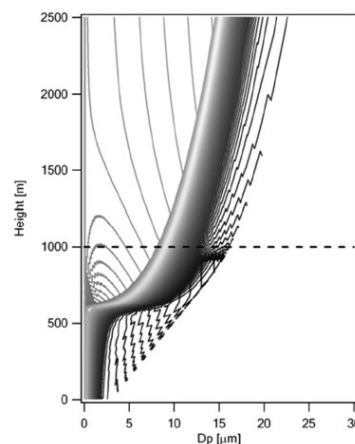
446

#### 447 **4. Elimination of air pollution by condensed water within a solar chimney**

448 Since the pollutants in the air were eliminated by spraying water in the chimney  
449 at the expense of water loss, this section introduces one variation of solar chimney  
450 sourcing the water to be sprayed from the air itself. Water droplets can be formed under  
451 certain conditions from vapor in the air and can be used to scavenge air pollutants.

##### 452 **4.1 The mechanism of fine aerosol removal by condensed water**

453 As the air temperature declines with the increase in altitude, if the air ascends in  
454 the chimney and reaches its saturation point due to the temperature drop, water vapor  
455 begins to condense into cloud droplets, coalesce, grow, and become precipitation. This  
456 precipitation would have the scavenging function as the natural rain to eliminate  
457 pollution in the air. It was found that if the air humidity at the entrance of the chimney  
458 was maintained at 80%, the saturation point could be reached within the chimney of  
459 500 m and 700 m, and the droplets from vapor were formed. At the top of the chimney  
460 (1000 m), some droplets had grown to 15  $\mu\text{m}$  in diameter ( $D_p$  in Fig. 10,  $\mu\text{m}$ )  
461 (VanReken and Nenes, 2009). But if a higher chimney was provided, the diameter of  
462 the droplets would be increased to the 25-30  $\mu\text{m}$  diameter threshold, beyond which a  
463 large scale of coalescence occurs, leading to the drizzle rapid formation process (light  
464 rainfall) (Sauvageot, 1995).



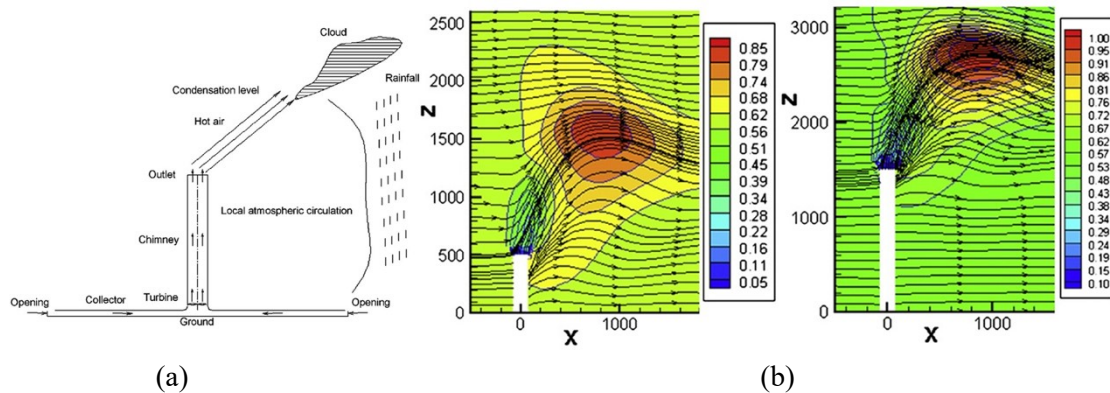
465

466 Fig. 10. Cloud droplet evolution in a chimney (cloud formation from ~600 m above and the  
467 top of the chimney is shown by a dashed line) (VanReken and Nenes, 2009).

468 This theory of artificial rain was also analyzed by Zhou et al. (2008). Since the air

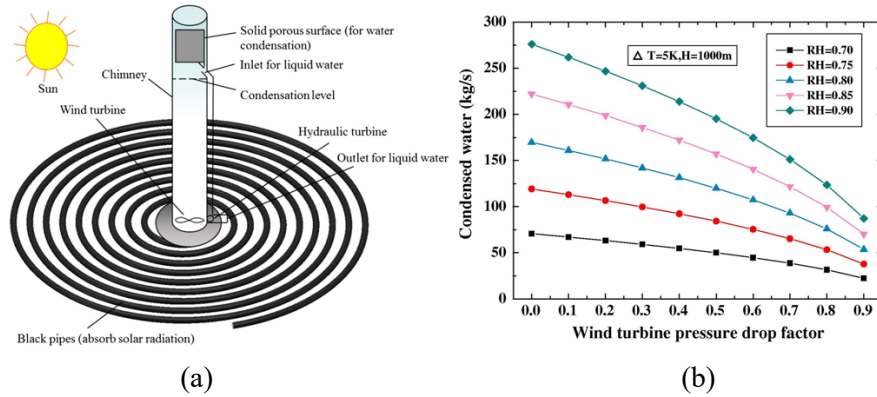


469 at the outlet of the chimney is still warmer and lighter than the ambient air, this air will  
 470 rise above the chimney until the temperature difference between the airflow and the  
 471 surrounding air (or the relative velocity) becomes zero. During the rise, the temperature  
 472 of airflow drops due to the adiabatic cooling, and its relative humidity increases, then  
 473 rainfall may be formed after the 100% relative humidity is reached (see Fig. 11a). A  
 474 numerical simulation of this artificial rainfall theory was made to validate this concept  
 475 (see Fig. 11b) (Zhou et al., 2009a). The horizontal and vertical axis in this figure shows  
 476 the horizontal distance from the chimney (m) and the altitude (m), respectively. The  
 477 white column is the chimney and the color vertical bar on the right side indicates the  
 478 variation of relative humidity. It was shown that a higher chimney had a larger chance  
 479 to make the plume reach the saturation point. It was also claimed that this artificial  
 480 climate can support agriculture in the arid region (e.g. the large parts of North and West  
 481 China) and may rehabilitate the desert lands (Zhou et al., 2010). This rainfall will also  
 482 support the purpose of air pollution elimination.



483  
 484 (a) (b)  
 485 Fig. 11. Artificial rainfall formed by the solar chimney, (a) schematic illustration (Zhou et al.,  
 486 2008), and (b) the simulation results (Zhou et al., 2009a).

487 To collect the condensed water vapor at a lower height and more efficiently, a  
 488 solid porous surface condenser mounted on the top of a chimney (above the saturation  
 489 point level) was proposed (Ming et al., 2017) and shown in Fig. 12. The vapor in the  
 490 air will condense and adhere to these solid porous surfaces and be collected underneath  
 491 the solid porous surface by gravity. More than 100 kg/s condensed water could be  
 492 collected in a 1000 m high chimney with 100 m in diameter when the relative humidity  
 493 of ambient air is 0.70. At the same time, the mass flow rate of air driven into the  
 494 chimney is 14 m/s. More water will be generated from the air with higher relative  
 495 humidity, see Fig. 12b. This water collected by the condenser will not go to the  
 496 hydraulic turbines and the wind turbine will not work when it is used for air treatment.  
 497 The black pipes are for the storage of solar energy during the daytime.

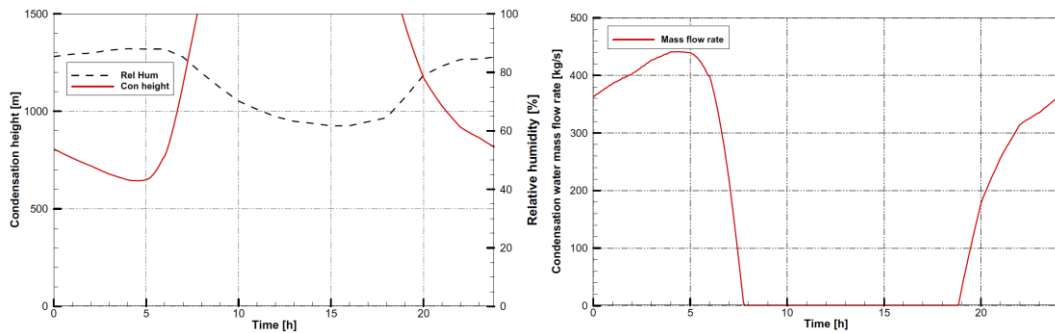


498  
499

500 Fig. 12. A chimney with a condensation device, (a) schematic design, (b) the production rate  
501 of condensed water (Ming et al., 2017).

502  
503  
504  
505  
506  
507  
508  
509  
510  
511  
512

The seasonal and diurnal variation in vapor condensation performance were studied and analyzed under Wuhan's moist climate conditions in a 1500 m chimney (Xu et al., 2015). Fig. 13 shows the condensation height (saturation point level) and daily condensed water mass flow rate varied in this chimney over 24 h in Wuhan on a typical summer day (July 21). The condensation level in the chimney varied with the ambient air humidity, with condensation occurring from about 6:50 pm to 7:50 am and no condensation at other times due to the relatively low humidity. The lowest condensation height was about 644.07 m, while the maximum condensation water mass low rate could reach to 450 kg/s, which is comparable with the water loss of a cooling tower for the 500 MW power plant and much larger than the water needs for spray in the solar chimney proposed by Akbarzadeh (see section 3).



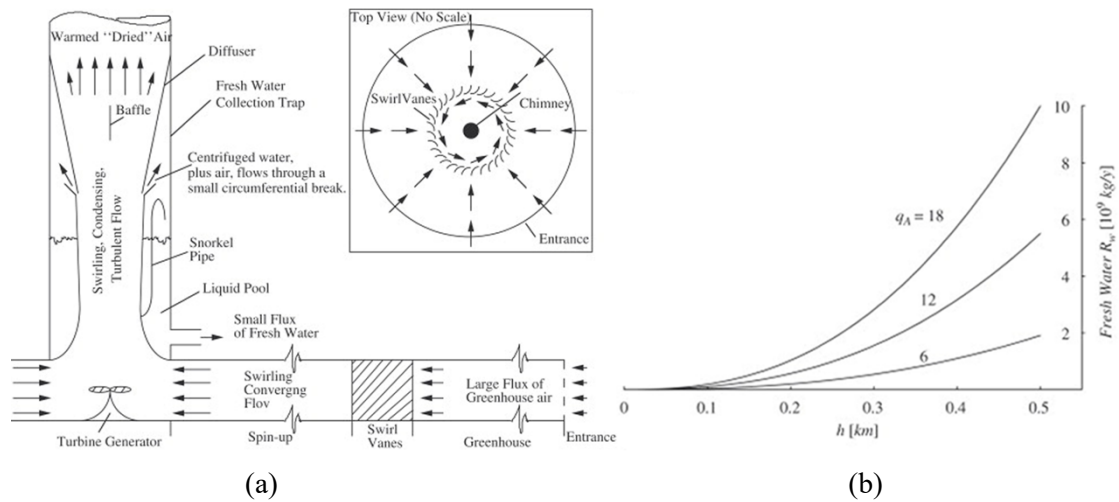
513  
514  
515

516 Fig. 13. (a) Daily variation of the condensation height, and (b) Daily condensation water mass  
517 flow rate (Xu et al., 2015).

518  
519  
520  
521  
522  
523  
524

A solar cyclone (a variation of the solar chimney, see Fig. 14) was introduced to harvest water from the atmosphere (Kashiwa and Kashiwa, 2008). The swirl vanes that were set in the path of the air moving towards the chimney induced the radial flow of air (from the periphery to the center) to spin. Both the radial and swirl part of velocity rise when the airflow path contracts from the canopy to the chimney. The temperature of the air will drop with the velocity increase due to conservation. The air temperature reaches the lowest point (lower than the dew point of air) when the velocity gets its maximum at the turning point from horizontal to vertical and causes the condensation to happen. A separator was set at the bottom of the chimney to separate the condensed

525 water with air. For a 500m tall solar cyclone,  $6 \times 10^9$  kg/year (190 kg/s) water can be  
 526 generated from the air with 12.00 g/kg humidity ratio. It was also indicated in this paper  
 527 that the 12.00 g/kg humidity ratio is a typical value in many areas of populated Asia  
 528 where the serious haze may happen. That means the water generated by the solar  
 529 cyclone could cover the water loss caused by the spray system in the solar chimney.  
 530 Water production will increase with the rise of chimney height and the growth of  
 531 humidity ratio of the ambient air, see Fig. 14b.



532  
 533

534 Fig. 14. The solar cyclone, (a) the vapor condensation process, (b) water production rate  
 535 varied with the chimney height ( $h$ , km) and the humidity ratio ( $q_A$ , g/kg) (Kashiwa and  
 536 Kashiwa, 2008).

#### 537 4.2 Evaluation of the condensed water measure

538 To promote the economic feasibility of this geoengineering measure, many  
 539 innovations were proposed to reduce the construction and operational cost of the huge  
 540 chimney system. Due to the large proportion of initial investment of the canopy (Ming  
 541 et al., 2016b), Bonnelle (2004) proposed a solar chimney with no canopy, using the  
 542 condensation latent heat of the vapor in the updraft airflow as the driving force (see Fig.  
 543 15). When the updraft airflow reaches the saturation point level in the chimney, the  
 544 vapor condensation would happen in the air which could emit the latent heat and heat  
 545 the air. This heat from the air itself was used to substitute for the heat gained from the  
 546 canopy. This procedure can be self-sustained and with no additional energy needed,  
 547 similar to natural convective processes (Wu et al., 2020). As stated by Kashiwa and  
 548 Kashiwa (2008), the temperature rise generated by vapor condensation in the arid  
 549 region would reach 10 K. While the temperature rises from a canopy with 244m in  
 550 diameter at Manzanares, Spain is only 15 K.

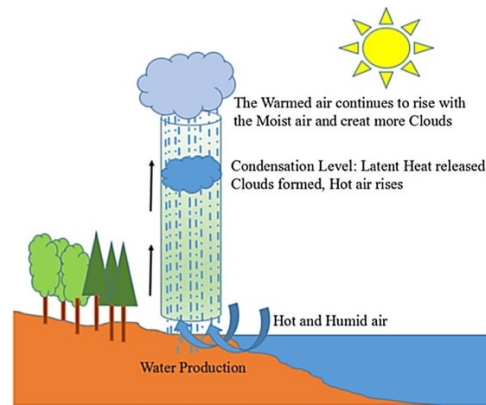


Fig. 15. The process of water vapor condensation in a chimney without canopy (Ming et al., 2016b)

The ideas of using heat discharged by power plants or from natural geothermal energy as the driving force in the solar chimney instead of the canopy have also been proposed and studied by several research teams (Cao et al., 2014; Chen et al., 2014; Fathi et al., 2018; Hu and Leung, 2017). By using this essentially free energy, these solar chimneys have almost no operational costs with condensation in the chimney occurring.

Some of the chimneys proposed in this study are quite high, but several articles from NASA (U.S.) describe the feasibility of chimneys several kilometers tall, and patents on this high conduit for aerosol spraying have been approved in many countries (Ming et al., 2014). Bolonkin (2011) even proposed a 3 km high chimney made from inexpensive inflatable tubes to harvest fresh water from the atmosphere. It was claimed that the water production could be  $7.86 \times 10^7 \text{ m}^3/\text{year}$  at the initial construction cost of 20 million dollars and  $4 \text{ km}^2$  land.

To summarize, it is demonstrated that the water needed in the spray system to scavenge the air pollution can be harvested from the air itself at a high place in the chimney (except the solar cyclone). More water will be generated in the humid region. Although the initial investments of a tall chimney are large, it is pointed out that the solar chimney method is the only method that can produce water and induce air simultaneously on a large scale compared with sorption methods, condensation method using vapor compression cycle, the desiccant wheel method, and membrane assisted methods (Tu and Hwang, 2020).

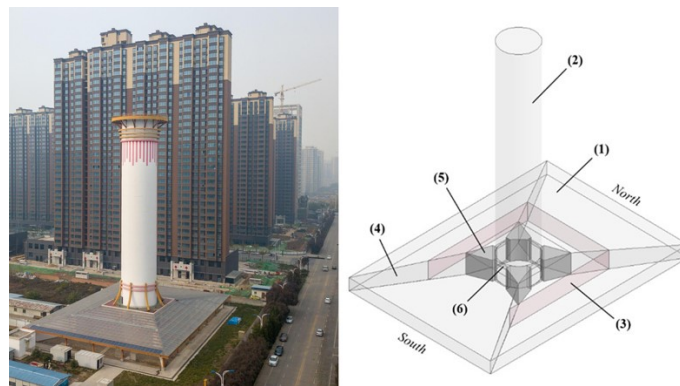
## 5. Elimination of air pollution by a filter within a solar chimney

A significant amount of water is needed in the water spraying approach. For the megacities that are plagued by water scarcity and haze events simultaneously, another alternative measure to eliminate aerosols in the air by a filter in a solar chimney is proposed and discussed in this section.

### 5.1 The mechanism of filter measure

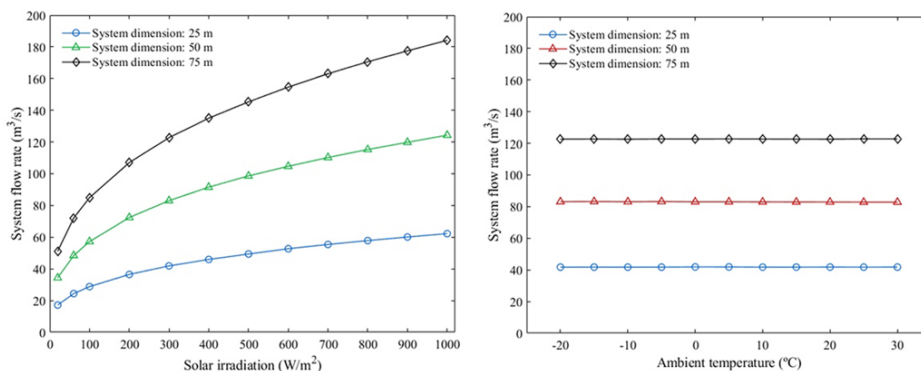
582 Utilizing the chimney effect to suck the polluted air and channel the air through  
 583 filters is proposed (<http://www.except.nl/en/>, accessed on 12 October 2020), which is  
 584 similar to the giant vacuum cleaners. A concept of a solar-assisted large-scale cleaning  
 585 system (SALSCS), which was a variation of the solar chimney, was proposed to filter  
 586 the polluted air (Cao et al., 2015). This SALSCS for air pollution abatement included a  
 587 500 m chimney with filter banks mounted under the solar radiation canopy. Its air  
 588 processing capability was claimed up to be  $2.64 \times 10^5 \text{ m}^3/\text{s}$ .

589 To investigate the real air pollutant removal ability and the efficiency of the  
 590 SALSCS, a prototype (see Fig. 16) is built in the downtown of Xi'an, China. It has a  
 591  $43 \times 60 \text{ m}^2$  solar radiation canopy and a 60 m high chimney (Cao et al., 2018b). The  
 592 initial cost of this prototype was US\$2 million (Cyranoski, 2018). The filtration  
 593 efficiency for PM<sub>2.5</sub> obtained reached 73.5% on average, with the rate of airflow  
 594 reaching  $35 \text{ m}^3/\text{s}$ . According to released experiment data, PM<sub>2.5</sub> concentration in the  
 595 air within the  $10 \text{ km}^2$  surrounding area would be reduced by 15%, which means it would  
 596 benefit about 300 thousand nearby people (<https://www.sohu.com/picture/277749907>,  
 597 accessed on 12 October 2020).



598  
 599 Fig. 16. The picture of SALSCS and its schematic design with (1) solar collector, (2) tower,  
 600 (3) filters, (4) partition walls, (5) storage room, and (6) rolling doors (Cao et al., 2018b).

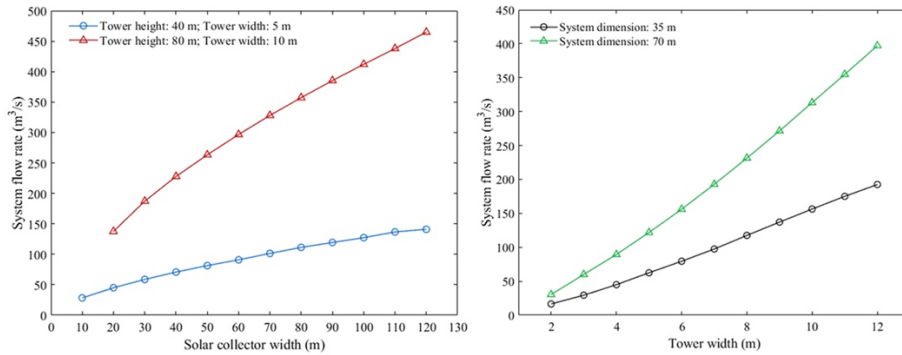
601 The performance of this air filter system is affected by the weather condition. As  
 602 displayed in Fig. 17, a higher solar radiation flux will induce more air into the system.  
 603 However, the temperature of the surrounding air has little influence on the airflow rate  
 604 of the system.



605  
 606 Fig. 17. Performance of SALSCS affected by the weather condition, (a) solar irradiation, (b)  
 607 ambient temperature (Cao et al., 2018a)



608 The performance of this air filter system is also affected by the configurations.  
 609 From Fig. 17, a higher chimney will suck more air into the chimney (system dimension  
 610 indicates the height of the chimney). A larger collector and a wider chimney will be  
 611 beneficial for the performance, see Fig. 18.



612  
 613 Fig. 18. Performance of SALSCS affected by the configurations, (a) solar collector width, (b)  
 614 tower width (Cao et al., 2018a)

## 615 5.2 Evaluation of this filter measure

### 616 5.2.1 Discussion of the solar chimney used in the filter measure

617 One problem with those filter systems based on solar chimney is its low efficiency.  
 618 The kinetic energy of the air current in the chimney is converted from the heat gains  
 619 obtained from the solar radiation. The energy conversion efficiency that defined as the  
 620 ratio of the kinetic energy to the solar radiation is expressed as (Zhou and Xu, 2016):

$$621 \quad \eta = \eta_{ch} \cdot \eta_{coll} = \frac{gH_{ch}}{c_p T_{in}} \cdot \frac{c_p m (T_{out} - T_{in})}{A_{coll} S_g} \quad (1)$$

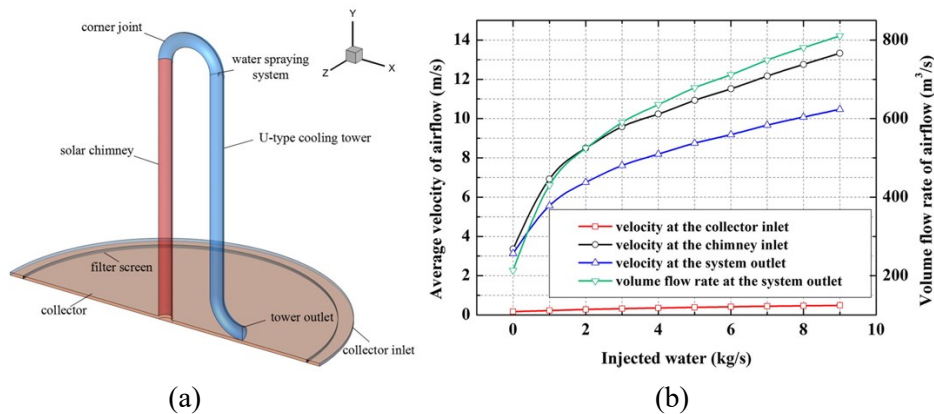
622 where the  $\eta_{ch}$  is the chimney efficiency (the ratio of the kinetic energy of the air to  
 623 the heat gains),  $\eta_{coll}$  is the solar collector efficiency (the ratio of heat gains of the air  
 624 to the solar radiation),  $H_{ch}$  is the height of the chimney (m),  $c_p$  is the constant-  
 625 pressure specific heat of air (J/kg · K),  $A_{coll}$  is the area of the collector (m<sup>2</sup>),  $S_g$  is the  
 626 global solar radiation (W/m<sup>2</sup>),  $T_{in}$  and  $T_{out}$  is the air temperature at the inlet and  
 627 outlet of the collector (K), and  $m$  is the mass flow rate of air (kg/s). The  $\eta_{coll}$  is  
 628 approximately 32% for the Spanish prototype (Guo et al., 2019). One can easily  
 629 calculate the  $\eta_{ch}$  and conclude that this efficiency is lower than 5% for a 1000m  
 630 chimney.

631 To increase the efficiency of the solar chimney and induce more air into the system  
 632 at fixed solar radiation, Huang et al. (2020a) proposed a system based on the SALSCS,  
 633 but the glass canopy under the chimney was replaced by photovoltaic panels. The  
 634 photovoltaic panels were used to generate power to drive suction fans and propel the  
 635 air into the chimney. A 194.6 m high chimney with 113 m glass canopy in diameter  
 636 could induce 975.93 m<sup>3</sup>/s air into the chimney. While, when the entire top surface of  
 637 the canopy was replaced by photovoltaic panels, the total air flow rate would increase  
 638 to 2.21 times. The mass rate of airflow is lower due to the shade effects of the  
 639 photovoltaic panels but increased by the electricity generated by those panels. This

640 output was achieved by the combined efforts of the chimney and photovoltaic panels.  
 641 Without the cooling effects of the airflow in a chimney, the efficiency of photovoltaic  
 642 panels will deteriorate due to their temperature rise (Jamali et al., 2019).

643 Another problem with the filter system is that the clean air driven out of the  
 644 chimney ascended into the upper level of the atmosphere and not to the level where  
 645 human activity takes place. The average mass mixing ratio of filtered air with the  
 646 atmosphere below 50 m (from the surface of the Earth) reached only  $5.22 \times 10^{-3}$  (kg/kg  
 647 dry-air) (Cao et al., 2018c). A higher chimney could drive more polluted air in but may  
 648 result in even less filtered air reaching the breath area due to the longer mix distance  
 649 and a higher outlet air velocity.

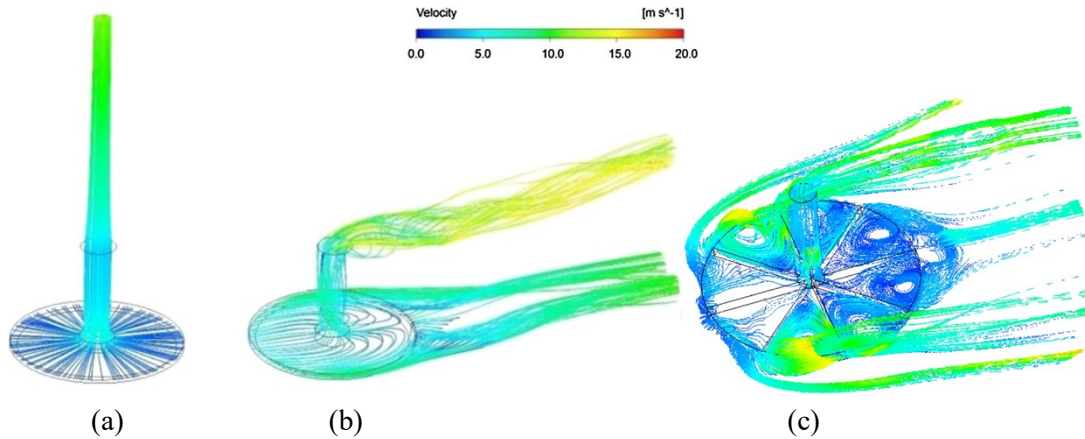
650 To address this problem, a novel 200 m solar chimney cooling tower combined  
 651 system was proposed by Gong et al. (2017) and shown in Fig. 19. The hot air heated by  
 652 the solar collector travels through the filter screen and rises in the solar chimney due to  
 653 buoyancy. When it moves through the corner joint, the air will be cooled by the water  
 654 spraying system. This cooled air will become denser and heavier than the air in the  
 655 chimney and drag the air from the chimney to the cooling tower. Fig. 19b presents that  
 656 the volume rate of air sucked into the system is more than the volume rate without a  
 657 spraying system. When more water is injected by the spraying system, the air becomes  
 658 further cooled and heavier. This gives a larger air pressure difference between the  
 659 pressure in the chimney and the tower, which will drive more polluted air into the  
 660 system to be purified.



661  
 662 (a)  
 663 Fig. 19. The solar chimney cooling tower combined system, (a) 3-D model, (b) the variation  
 664 of volume flow rate and the velocity of airflow (Gong et al., 2017).

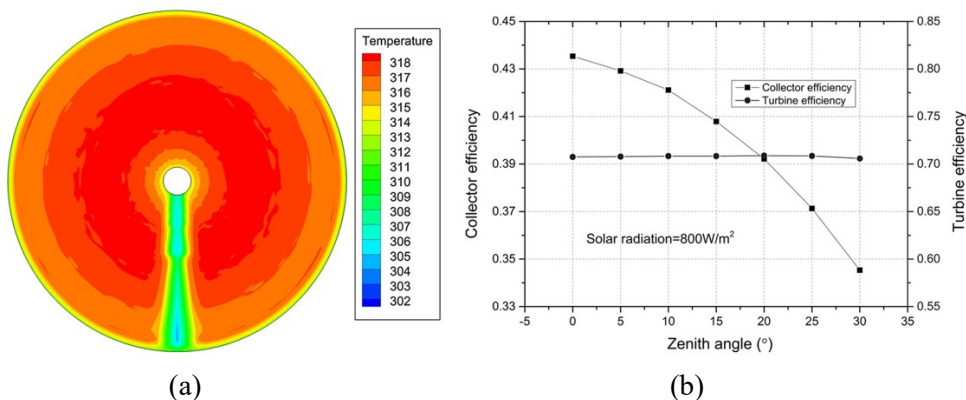
665 The airflow in the solar chimney is also affected by the crosswind, which is shown  
 666 in Fig. 20. The simulation concluded that the crosswind near the outlet of the chimney  
 667 would compel the flow to incline and hinder the updraft to flow out. While, the  
 668 crosswind near the inlet of the canopy would blow the hot air heated by the canopy out  
 669 of the canopy and hamper its converge at the bottom of the chimney (Zou et al., 2017).  
 670 See Fig. 20a and Fig. 20b. The state of the flow pattern would be improved in the same  
 671 chimney but with union-jack-shaped windbreak walls under the canopy because parts  
 672 of the wind were blocked by walls and forced to enter into the chimney, see Fig. 20c.

673 It was claimed that this system would filter the particles out from the air driven into the  
 674 chimney at the rate of 3.5 kg/h when the concentration of particles was  $500 \mu\text{g}/\text{m}^3$  and  
 675 the filter efficiency was 0.8 (Zhu et al., 2019).



676  
 677 (a) (b) (c)  
 678 Fig. 20. Airflow pattern of a solar chimney affected by the crosswind, (a) no wind, (b)  
 679 crosswind velocity is 10 m/s (Zou et al., 2017), and (c) crosswind velocity is 10 m/s with  
 680 windbreak walls (Zhu et al., 2019).

681 Since the driving force of the airflow is the heat gained from the canopy, the  
 682 canopy (collector) efficiency (which is defined as the ratio of the solar energy gained  
 683 by the air to the solar radiation flux) affected by the solar zenith angle will have an  
 684 impact on the performance of the solar chimney (Guo et al., 2015). If the solar radiation  
 685 flux is fixed, the collector efficiency will decrease with the solar zenith angle increase  
 686 because of the shade effects of the tall-and-opaque chimney on the collector (the angle  
 687 is  $0^\circ$  when the radiation is aligned with the chimney). From Fig. 21a, the temperature  
 688 of the collector roof shaded by the chimney was much lower than other parts of the  
 689 collector roof when the solar zenith angle was set to be  $30^\circ$ . The variation of collector  
 690 efficiency with the solar zenith angle was depicted in Fig. 21b. With the zenith angle  
 691 increasing, the collector efficiency will decrease, thus the rate of airflow driven into the  
 692 chimney will reduce.



693  
 694 (a) (b)  
 695 Fig. 21. The shade effect of the chimney on the collector, (a) temperature variation on a  
 696 collector roof, and (b) efficiency variation with the solar zenith angle (Guo et al., 2015).

### 697 5.2.2 Discussion of the filter technology

698 The filter technologies described here require some advances to be commercially



699 viable. First, a filter's efficiency and holding capacity (the maximum dust that can be  
700 gathered during the service life of a filter) can vary against different particle size  
701 distributions (Chang et al., 2019). The holding capacity of the filters treating fine  
702 particles was lower compared with the coarse particle filter process (Tang et al., 2018).  
703 Since the chemical and physical components of air pollution will be distinct in different  
704 places and different seasons (Jiang et al., 2018), custom filters need to be developed for  
705 specific systems to maintain efficiency at a reasonable level.

706 Second, traditional commercial air filters could not filter out the precursors to  
707 particulate matter (e.g., sulfur dioxide gas and nitrogen oxides), which resulted in  
708 visually clear air but poor air quality. To remedy this issue, a metal-organic air filter  
709 modified by carbon nanotube was produced for ultrafine particle filtration and SO<sub>2</sub>  
710 absorption (Feng et al., 2018). A kind of air filter made by biodegradable cellulose was  
711 developed, which has fine filtration efficiency and antibacterial capability (Ma et al.,  
712 2019).

713 Lastly, most of the commercial air filters are fabricated from petroleum-based  
714 materials with low degradability, which may also become solid pollutants after usage  
715 (Ma et al., 2019). A kind of environment-friendly and high-efficient material needs to  
716 be developed for the solar chimney. Though a new porous material made from calcium  
717 iodate, sodium alginate, and silica fume was proposed for air particle collection  
718 (Zanoletti et al., 2018), which can be regenerated by rainfall. It still needs to be tested  
719 in a large-scale application in further research.

720

## 721 **6. Overview of the air pollution removal techniques proposed**

722 To put those air pollution removal techniques based on the solar chimney in  
723 practice, the economic aspects need to be considered. The investment always contains  
724 the chimney cost, the canopy cost, and the land cost. Though the measure of pollution  
725 scavenged by the sprayed water droplet may not need the canopy, it needs a reservoir  
726 to store the water. The cost of a solar chimney was reviewed by Zhou and Xu (2016).  
727 The chimney cost varied from 175.4 to 419 €/m<sup>2</sup>, which was calculated by dividing the  
728 chimney cost by the superficial area of the chimney assumed in a cylindrical shape. The  
729 canopy cost varied from 7.27 to 34.22 €/m<sup>2</sup>, which was calculated by dividing the  
730 collector cost by the collector area. The cost depends on the construction time,  
731 construction site, and physical size of the solar chimney. Most of those solar chimneys  
732 for power generation were proposed to be built in the desert or mountainous regions,  
733 the land cost was always neglected. However, those measures aimed at air pollution  
734 removal should be built in the city in which the land cost will be higher. For reference,  
735 the price of Class III land (the land is divided by five classes, Class I is near the  
736 downtown) for the industry is about 1,000 RMB/m<sup>2</sup> ( $\approx$ 143 \$/m<sup>2</sup>) in Wuhan, the largest  
737 city in Central China (<http://www.whdsc.com/jzdj/10391.jhtml>, accessed on 12  
738 October 2020). For the spray measures without a canopy, the price of a water supply

739 and spray system including a 1,000,000 m<sup>3</sup> reservoir is about 59.8 million dollars  
740 (Altmann et al., 2005). Since the water collected after the air pollution scavenging  
741 process by spraying has a similar property as the rainwater, a natural reservoir (pond,  
742 lake, or river) may be used to save cost. Although a huge initial investment is needed  
743 for the construction of an air-purification system based on the solar chimney, the  
744 achievable health benefits (lower premature mortality and reductions in hospital  
745 admissions for respiratory issues) cannot be weighted by monetary terms.

746 Table 3 shows the key innovation and strengths of those four geoengineering  
747 measures based on the solar chimney reviewed in this paper. Those measures not only  
748 can handle pollutions in the air at low operational expense without large-scale negative  
749 impacts on the environment but also can be controlled by human beings without waiting  
750 for a special weather condition. Though none of those geoengineering measures is  
751 perfect for managing air pollution at this stage, they do provide health benefits for the  
752 public and they also propose a starting point and a platform to develop a more economic,  
753 more efficient and smaller environmental impact measure in the future.

**Table 3****Comparison of Air Pollution Removal Measures**

Measures	Technological novelty	Strengths and weaknesses	Environmental impacts	Requirements and costs
High solar chimney	Utilizing the heat island effect or solar energy to avoid the dramatic growth of PM2.5 and haze formation (Zhong et al., 2019a).	It opens the meteorological channels for pollution dispersion, preventing the “two-way feedback mechanism” (Miao et al., 2018; Zhong et al., 2019b), but cannot eliminate pollution physically.	The uplifted air pollution may be transported to a long distant location (Langford et al., 2010; Minoura et al., 2016).	A chimney must be higher than PBL (Zhou et al., 2015); a floating chimney could be feasible and more economical (Papageorgiou, 2007; Zhou and Yang, 2009; Zhou et al., 2009b).
Solar chimney with water spraying	Combining the large-scale scavenging effect of spraying and the ability to generate power.	It can remove particles in the air (Cui et al., 2017; Wang et al., 2010; Yu, 2014) at a relatively low water loss (Akbarzadeh et al., 2009).	Water loss; The water collected after scavenge could be treated as natural rainwater.	A high chimney, pumps, spray system and sufficient water resources are needed (Akbarzadeh et al., 2009).
Solar chimney with condensed water from vapor in the air	The water for scavenging particles can be harvested from the air itself.	The water harvested from the air itself can satisfy the need in the spraying system to scavenge the air pollution (Kashiwa and Kashiwa, 2008; Ming et al., 2017).	Improve the climate near the chimney (Zhou et al., 2010). The water collected after scavenge could be treated as natural rainwater.	A high chimney is needed (Ming et al., 2017; Xu et al., 2015).

754

755

756

757

**Table 3 (continued)**

**Comparison of Air Pollution Removal Measures**

Measures	Technological novelty	Strengths and weaknesses	Environmental impacts	Requirements and costs
Solar chimney with air filter	Using solar energy to drive the polluted air through air filters.	Not only filter aerosol(Cao et al., 2015; Cao et al., 2018c) but also eliminate acid gas pollutants (Feng et al., 2018); Some filters can be regenerated by rain (Zanoletti et al., 2018).	Filters may need to be replaced regularly; those petroleum-based filters are not degradable (Ma et al., 2019).	A chimney; Tailored filters for specific air pollutants (Jiang et al., 2018).

759 **7. Discussion and conclusion**

760 With the continuous economic growth and rapid industrialization of many  
761 developing countries with high populations (e.g., China and India), governments and  
762 the general public encounter the growing air pollution problems (particularly the  
763 serious PM problem) and determine to address these issues. The haze caused mainly by  
764 particles, which has negative impacts on human health and leads to unsustainable  
765 regulation of transportation and high-polluting industries, must be overcome in the  
766 coming years.

767 The fundamental solution to the PM problem is to replace fossil fuels with clean  
768 and renewable energy. However, we cannot wait for the day when fossil fuels are  
769 completely phased out and do nothing at present time. To relieve the harmful effects of  
770 PM on the health of the general public in the near term, several geoengineering  
771 measures based on solar chimneys were reviewed in this article. They have the large-  
772 scale elimination ability on pollutants in the air, particularly for particulate matter. The  
773 measures include driving the polluted air penetrate the planetary boundary layer into  
774 the troposphere to avoid the dramatic growth of concentrations of particulate matter,  
775 spraying water on the top of the chimney into the air to scavenge pollution, and  
776 intercepting fine particles in the air driven by the chimney with large filters.

777 Compared with traditional methods (e.g., emission control at sources, giant spray  
778 trucks), those solar chimney geoengineering measures have the following advantages:  
779 1) They can be operated 24 hours a day and thus keep the pollution removal function  
780 stable and continuous. 2) They are environment-friendly measures, which can generate  
781 clean electricity by turbines from the airflow to compensate for the consumption of  
782 energy that is most likely from fossil fuels in the developing countries and thus reduce  
783 emissions. 3) They are also robust, need very low maintenance and can work for a long  
784 time. After reimbursement of the initial investment, those geoengineering measures  
785 could generate power at low operational costs.

786 Given the advantages of the solar chimney geoengineering measures and the  
787 economic and human health losses caused by air pollution, those geoengineering  
788 approaches deserve to be studied further and implemented in those countries that are  
789 suffering from the heavy air pollution issue.

790

791 **Acknowledgments:**

792 This study was financially supported by the National Natural Science Foundation of  
793 China (Grant No. 51778511, 51778253), a European Commission H2020 Marie S  
794 Curie Research and Innovation Staff Exchange (RISE) award (Grant No. 871998), the  
795 Hubei Provincial Natural Science Foundation of China (Grant No. 2018CFA029), and

796 the Key Project of ESI Discipline Development of Wuhan University of Technology  
797 (WUT Grant No. 2017001).

798

799 **References**

800 Akbarzadeh A, Johnson P, Singh R. Examining potential benefits of combining a chimney with  
801 a salinity gradient solar pond for production of power in salt affected areas. *Solar Energy* 2009;  
802 83: 1345-1359.

803 Altmann T, Carmel Y, Guetta R, Zaslavsky D, Doytsher Y. Assessment of an “Energy Tower”  
804 potential in Australia using a mathematical model and GIS. *Solar Energy* 2005; 78: 799-808.

805 Bauer M, Gasser I. Modeling, Asymptotic Analysis, and Simulation of an Energy Tower. *SIAM*  
806 *Journal on Applied Mathematics* 2012; 72: 362-381.

807 Blanco-Alegre C, Castro A, Calvo AI, Oduber F, Alonso-Blanco E, Fernández-González D, et  
808 al. Below-cloud scavenging of fine and coarse aerosol particles by rain: The role of raindrop  
809 size. *Quarterly Journal of the Royal Meteorological Society* 2018; 144: 2715-2726.

810 Bolonkin A. Production of Freshwater and Energy from Earth's Atmosphere. *Smart Grid and*  
811 *Renewable Energy* 2011; 02.

812 Bonnelle D. Solar Chimney, Water Spraying Energy Tower, and Linked Renewable Energy  
813 Conversion Devices: Presentation, Criticism and Proposals. France: University Claude Bernard;  
814 2004.

815 Brancher M, Griffiths KD, Franco D, de Melo Lisboa H. A review of odour impact criteria in  
816 selected countries around the world. *Chemosphere* 2017; 168: 1531-1570.

817 Burnett RT, Pope CA, Ezzati M, Olives C, Lim SS, Mehta S, et al. An Integrated Risk Function  
818 for Estimating the Global Burden of Disease Attributable to Ambient Fine Particulate Matter  
819 Exposure. *Environmental Health Perspectives* 2014; 122: 397-403.

820 Cao F, Li H, Ma Q, Zhao L. Design and simulation of a geothermal–solar combined chimney  
821 power plant. *Energy Conversion and Management* 2014; 84: 186-195.

822 Cao Q, Huang M, Kuehn TH, Shen L, Tao W-Q, Cao J, et al. Urban-scale SALSCS, Part II: A  
823 Parametric Study of System Performance. *Aerosol and Air Quality Research* 2018a; 18: 2879-  
824 2894.

825 Cao Q, Kuehn TH, Shen L, Chen S-C, Zhang N, Huang Y, et al. Urban-scale SALSCS, Part I-  
826 Experimental Evaluation and Numerical Modeling of a Demonstration Unit. *Aerosol and Air*  
827 *Quality Research* 2018b; 18: 2865-2878.

828 Cao Q, Pui DYH, Lipiński W. A Concept of a Novel Solar-Assisted Large-Scale Cleaning  
829 System (SALSCS) for Urban Air Remediation. *Aerosol and Air Quality Research* 2015; 15: 1-  
830 10.

831 Cao Q, Shen L, Chen S-C, Pui DYH. WRF modeling of PM 2.5 remediation by SALSCS and  
832 its clean air flow over Beijing terrain. *Science of The Total Environment* 2018c; 626: 134-146.

833 Chang D-Q, Tien C-Y, Peng C-Y, Tang M, Chen S-C. Development of composite filters with  
834 high efficiency, low pressure drop, and high holding capacity PM2.5 filtration. *Separation and*  
835 *Purification Technology* 2019; 212: 699-708.

836 Chate DM, Murugavel P, Ali K, Tiwari S, Beig G. Below-cloud rain scavenging of atmospheric  
837 aerosols for aerosol deposition models. *Atmospheric Research* 2011; 99: 528-536.

838 Chen K, Wang J, Dai Y, Liu Y. Thermodynamic analysis of a low-temperature waste heat  
839 recovery system based on the concept of solar chimney. *Energy Conversion and Management*  
840 2014; 80: 78-86.

841 Chen Y, Zhao C, Zhang Q, Deng Z, Huang M, Ma X. Aircraft study of Mountain Chimney  
842 Effect of Beijing, China. *Journal of Geophysical Research* 2009; 114.

843 Cherrier G, Belut E, Gerardin F, Tanière A, Rimbert N. Aerosol particles scavenging by a  
844 droplet: Microphysical modeling in the Greenfield gap. *Atmospheric Environment* 2017; 166:  
845 519-530.

846 Cohen AJ, Brauer M, Burnett R, Anderson HR, Frostad J, Estep K, et al. Estimates and 25-year  
847 trends of the global burden of disease attributable to ambient air pollution: an analysis of data  
848 from the Global Burden of Diseases Study 2015. *The Lancet* 2017; 389: 1907-1918.

849 Cui H, Li N, Peng J, Cheng J, Zhang N, Wu Z. Modeling the particle scavenging and thermal  
850 efficiencies of a heat absorbing scrubber. *Building and Environment* 2017; 111: 218-227.

851 Cyranoski D. China tests giant air cleaner to combat urban smog. *Nature* 2018; 555: 152-153.

852 Ding AJ, Huang X, Nie W, Sun JN, Kerminen V-M, Petäjä T, et al. Enhanced haze pollution  
853 by black carbon in megacities in China. *Geophysical Research Letters* 2016; 43: 2873-2879.

854 Đorđević DS, Šolević TM. The contributions of high- and low altitude emission sources to the  
855 near ground concentrations of air pollutants. *Atmospheric Research* 2008; 87: 170-182.

856 EPA US. Basic Information about Visibility. 2020a. [https://www.epa.gov/visibility/basic-](https://www.epa.gov/visibility/basic-information-about-visibility)  
857 [information-about-visibility](https://www.epa.gov/visibility/basic-information-about-visibility). [accessed 13 March 2020]

858 EPA US. PM 2.5. 2020b. <https://www.epa.gov/pm-pollution>. [accessed 13 March 2020]

859 Fathi N, McDaniel P, Aleyasin SS, Robinson M, Vorobieff P, Rodriguez S, et al. Efficiency  
860 enhancement of solar chimney power plant by use of waste heat from nuclear power plant.  
861 *Journal of Cleaner Production* 2018; 180: 407-416.

862 Feng S, Li X, Zhao S, Hu Y, Zhong Z, Xing W, et al. Multifunctional metal organic framework  
863 and carbon nanotube-modified filter for combined ultrafine dust capture and SO<sub>2</sub> dynamic  
864 adsorption. *Environmental Science: Nano* 2018; 5: 3023-3031.

865 Finlayson-Pitts BJ, Pitts JN. CHAPTER 2 - The Atmospheric System. In: Finlayson-Pitts BJ,  
866 Pitts JN, editors. *Chemistry of the Upper and Lower Atmosphere*. Academic Press, San Diego,  
867 2000, pp. 15-42.

868 Fredericks S, Saylor JR. Parametric investigation of two aerosol scavenging models in the  
869 inertial regime. *Journal of Aerosol Science* 2016; 101: 34-42.

870 Gao Y, Ji H. Microscopic morphology and seasonal variation of health effect arising from  
871 heavy metals in PM<sub>2.5</sub> and PM<sub>10</sub>: One-year measurement in a densely populated area of urban  
872 Beijing. *Atmospheric Research* 2018; 212: 213-226.

873 Gong T, Ming T, Huang X, Renaudde\_Richter. Numerical analysis on a solar chimney with an  
874 inverted U-type cooling tower to mitigate urban air pollution. *Solar Energy* 2017; 147: 68-82.

875 Greenbaum D. Making measurable progress in improving China's air and health. *The Lancet*  
876 *Planetary Health* 2018; 2: e289-e290.

877 Greenfield SM. Rain Scavenging of Radioactive Particulate Matter from the Atmosphere.  
878 Journal of the Atmospheric Sciences 1956; 14: 115-125.

879 Guo P, Li J, Wang Y, Wang Y. Numerical study on the performance of a solar chimney power  
880 plant. Energy Conversion and Management 2015; 105: 197-205.

881 Guo P, Li T, Xu B, Xu X, Li J. Questions and current understanding about solar chimney power  
882 plant: A review. Energy Conversion and Management 2019; 182: 21-33.

883 He S, Gurgenci H, Guan Z, Hooman K, Zou Z, Sun F. Comparative study on the performance  
884 of natural draft dry, pre-cooled and wet cooling towers. Applied Thermal Engineering 2016;  
885 99: 103-113.

886 Hu D. Laboratory Study on Hygroscopicity and Optical Properties of Submicron Particles in  
887 Ambient Air: Fudan University; 2012.

888 Hu S, Leung DYC. Numerical Modelling of the Compressible Airflow in a Solar-Waste-Heat  
889 Chimney Power Plant. Energy Procedia 2017; 142: 642-647.

890 Hu XM. BOUNDARY LAYER (ATMOSPHERIC) AND AIR POLLUTION | Air Pollution  
891 Meteorology. In: North GR, Pyle J, Zhang F, editors. Encyclopedia of Atmospheric Sciences  
892 (Second Edition). Academic Press, Oxford, 2015, pp. 227-236.

893 Huang J, Pan X, Guo X, Li G. Health impact of China's Air Pollution Prevention and Control  
894 Action Plan: an analysis of national air quality monitoring and mortality data. The Lancet  
895 Planetary Health 2018a; 2: e313-e323.

896 Huang M-H, Chen L, Lei L, He P, Cao J-J, He Y-L, et al. Experimental and numerical studies  
897 for applying hybrid solar chimney and photovoltaic system to the solar-assisted air cleaning  
898 system. Applied Energy 2020a; 269: 115150.

899 Huang X, Ding A, Wang Z, Ding K, Gao J, Chai F, et al. Amplified transboundary transport of  
900 haze by aerosol–boundary layer interaction in China. Nature Geoscience 2020b; 13: 428-434.

901 Huang X, Wang Z, Ding A. Impact of Aerosol-PBL Interaction on Haze Pollution: Multi-Year  
902 Observational Evidences in North China. Geophysical Research Letters 2018b.

903 Health Effects Institute. State of Global Air 2018. A Special Report on Global Exposure to Air  
904 Pollution and Its Disease Burden. 2018.  
905 <http://www.stateofglobalair.org/sites/default/files/soga-2018-report.pdf>. [accessed 15 March  
906 2020]

907 Jafarifar N, Behzadi MM, Yaghini M. The effect of strong ambient winds on the efficiency of  
908 solar updraft power towers: A numerical case study for Orkney. Renewable Energy 2019; 136:  
909 937-944.

910 Jamali S, Nemati A, Mohammadkhani F, Yari M. Thermal and economic assessment of a solar  
911 chimney cooled semi-transparent photovoltaic (STPV) power plant in different climates. Solar  
912 Energy 2019; 185: 480-493.

913 Jiang N, Duan S, Yu X, Zhang R, Wang K. Comparative major components and health risks of  
914 toxic elements and polycyclic aromatic hydrocarbons of PM 2.5 in winter and summer in  
915 Zhengzhou: Based on three-year data. Atmospheric Research 2018; 213: 173-184.

916 Jose S, Gharai B, Kumar Y, Venkata P, Rao N. Radiative implication of a haze event over  
917 Eastern India. Atmospheric Pollution Research 2015; 6: 138-146.



918 Kang D, Strand RK. Performance control of a spray passive down-draft evaporative cooling  
919 system. *Applied Energy* 2018; 222: 915-931.

920 Kang Y, Hua F, Zhong K, Zhu H. A new analysis of fine aerosol capture by raindrops at  
921 terminal velocities. *Journal of Aerosol Science* 2015; 89: 31-42.

922 Kashiwa BA, Kashiwa CB. The solar cyclone: A solar chimney for harvesting atmospheric  
923 water. *Energy* 2008; 33: 331-339.

924 Koo J, Hong J, Lee H, Shin S. Effects of the particle residence time and the spray droplet size  
925 on the particle removal efficiencies in a wet scrubber. *Heat and Mass Transfer* 2010; 46: 649-  
926 656.

927 Kumar M. Global, regional, and national comparative risk assessment of 84 behavioural,  
928 environmental and occupational, and metabolic risks or clusters of risks for 195 countries and  
929 territories, 1990–2017: a systematic analysis for the Global Burden of Disease Study 2017. *The*  
930 *Lancet* 2018; 392.

931 Langford AO, Senff CJ, Alvarez RJ, Banta RM, Hardesty RM. Long-range transport of ozone  
932 from the Los Angeles Basin: A case study. *Geophysical Research Letters* 2010; 37.

933 Leffler RA, Bradshaw CR, Groll EA, Garimella SV. Alternative heat rejection methods for  
934 power plants. *Applied Energy* 2012; 92: 17-25.

935 Li P, Wang L, Guo P, Yu S, Mehmood K, Wang S, et al. High reduction of ozone and particulate  
936 matter during the 2016 G-20 summit in Hangzhou by forced emission controls of industry and  
937 traffic. *Environmental Chemistry Letters* 2017; 15: 709-715.

938 Li Q, Wu B, Liu J, Zhang H, Cai X, Song Y. Characteristics of the atmospheric boundary layer  
939 and its relation with PM<sub>2.5</sub> during haze episodes in winter in the North China Plain.  
940 *Atmospheric Environment* 2020; 223: 117265.

941 Li Z, Yu S, Wang L, Mehmood K, Liu W, Alapaty K. Suppression of convective precipitation  
942 by elevated man-made aerosols is responsible for large-scale droughts in north China.  
943 *Proceedings of the National Academy of Sciences* 2018; 115: E8327.

944 Liang J. 9 - Particulate matter. *Chemical Modeling for Air Resources*. Academic Press, Boston,  
945 2013, pp. 189-219.

946 Lin Y, Zou J, Yang W, Li C-Q. A Review of Recent Advances in Research on PM<sub>2.5</sub> in China.  
947 *International Journal of Environmental Research and Public Health* 2018; 15.

948 Liu L, Zhang X, Zhong J, Wang J, Yang Y. The ‘two-way feedback mechanism’ between  
949 unfavorable meteorological conditions and cumulative PM<sub>2.5</sub> mass existing in polluted areas  
950 south of Beijing. *Atmospheric Environment* 2019; 208: 1-9.

951 Liu XG, Li J, Qu Y, Han T, Hou L, Gu J, et al. Formation and evolution mechanism of regional  
952 haze: a case study in the megacity Beijing, China. *Atmospheric Chemistry and Physics* 2013;  
953 13: 4501-4514.

954 Lodhi MAK. Application of helio-aero-gravity concept in producing energy and suppressing  
955 pollution. *Energy Conversion and Management* 1999; 40: 407-421.

956 Lu X, Chan SC, Fung JCH, Lau AKH. To what extent can the below-cloud washout effect  
957 influence the PM<sub>2.5</sub>? A combined observational and modeling study. *Environ Pollut* 2019; 251:  
958 338-343.

959 Lu X, Yao T, Fung JCH, Lin C. Estimation of health and economic costs of air pollution over  
960 the Pearl River Delta region in China. *Sci Total Environ* 2016; 566-567: 134-143.

961 Ma S, Zhang M, Nie J, Tan J, Yang B, Song S. Design of double-component metal–organic  
962 framework air filters with PM<sub>2.5</sub> capture, gas adsorption and antibacterial capacities.  
963 *Carbohydrate Polymers* 2019; 203: 415-422.

964 Maia CB, Silva FVM, Oliveira VLC, Kazmerski LL. An overview of the use of solar chimneys  
965 for desalination. *Solar Energy* 2019; 183: 83-95.

966 Miao Y, Liu S, Guo J, Huang S, Yan Y, Lou M. Unraveling the relationships between boundary  
967 layer height and PM<sub>2.5</sub> pollution in China based on four-year radiosonde measurements.  
968 *Environmental Pollution* 2018; 243: 1186-1195.

969 Ming T, de\_Richter R, Liu W, Caillol S. Fighting global warming by climate engineering: Is  
970 the Earth radiation management and the solar radiation management any option for fighting  
971 climate change? *Renewable and Sustainable Energy Reviews* 2014; 31: 792-834.

972 Ming T, de\_Richter R, Shen S, Caillol S. Fighting global warming by greenhouse gas removal:  
973 destroying atmospheric nitrous oxide thanks to synergies between two breakthrough  
974 technologies. *Environmental Science and Pollution Research* 2016a; 23: 6119-6138.

975 Ming T, Gong T, de Richter RK, Wu Y, Liu W. A moist air condensing device for sustainable  
976 energy production and water generation. *Energy Conversion and Management* 2017; 138: 638-  
977 650.

978 Ming T, Gong T, Richter RKd, Liu W, Koonsrisuk A. Freshwater generation from a solar  
979 chimney power plant. *Energy Conversion and Management* 2016b; 113: 189-200.

980 Minoura H, Chow JC, Watson JG, Fu JS, Dong X, Yang C-E. Vertical Circulation of  
981 Atmospheric Pollutants near Mountains during a Southern California Ozone Episode. *Aerosol  
982 and Air Quality Research* 2016; 16: 2396-2404.

983 Omer E, Guetta R, Ioslovich I, Gutman PO, Borshchevsky M. “Energy Tower” combined with  
984 pumped storage and desalination: Optimal design and analysis. *Renewable Energy* 2008a; 33:  
985 597-607.

986 Omer E, Guetta R, Ioslovich I, Gutman PO, Borshchevsky M. Optimal Design of an “Energy  
987 Tower” Power Plant. *IEEE Transactions on Energy Conversion* 2008b; 23: 215-225.

988 Papageorgiou C. Floating Solar Chimney versus Concrete Solar Chimney Power Plants. 2007  
989 International Conference on Clean Electrical Power. IEEE, 2007, pp. 760-765.

990 Papageorgiou C. Floating Solar Chimney Technology: A Solar Proposal for China. *Proceedings  
991 of ISES World Congress 2007 (Vol. I – Vol. V)*, 2008, pp. 172-176.

992 Pöschl U. Atmospheric Aerosols: Composition, Transformation, Climate and Health Effects.  
993 *Angewandte Chemie International Edition* 2005; 44: 7520-7540.

994 Quan J, Gao Y, Zhang Q, Tie X, Cao J, Han S, et al. Evolution of planetary boundary layer  
995 under different weather conditions, and its impact on aerosol concentrations. *Particuology* 2013;  
996 11: 34-40.

997 Rong L, Turco RP. Ozone distributions over the los angeles basin: Three-dimensional  
998 simulations with the smog model. *Atmospheric Environment* 1996; 30: 4155-4176.

999 Rosenfeld D, Zhu Y, Wang M, Zheng Y, Goren T, Yu S. Aerosol-driven droplet concentrations  
1000 dominate coverage and water of oceanic low level clouds. *Science* 2019; 363: eaav0566.

1001 Roy A, Chatterjee A, Ghosh A, Das SK, Ghosh SK, Raha S. Below-cloud scavenging of size-  
1002 segregated aerosols and its effect on rainwater acidity and nutrient deposition: A long-term  
1003 (2009–2018) and real-time observation over eastern Himalaya. *Science of The Total*  
1004 *Environment* 2019; 674: 223-233.

1005 Sauvageot H. *Microphysical processes in clouds* : K.C. Young, 1993. Oxford University Press,  
1006 427 pp. Price: £45 Hardback. ISBN 0-19-507563-3. *Atmospheric Research* 1995; 39: 261.

1007 Schlaich Jr, Bergermann R, Schiel W, Weinrebe G. Design of Commercial Solar Updraft Tower  
1008 Systems—Utilization of Solar Induced Convective Flows for Power Generation. *Journal of*  
1009 *Solar Energy Engineering* 2005; 127: 117-124.

1010 Seinfeld, JH, Pandis. *Atmospheric chemistry and physics: From air pollution to climate change*,  
1011 2006.

1012 Song C, He J, Wu L, Jin T, Chen X, Li R, et al. Health burden attributable to ambient PM2.5  
1013 in China. *Environmental Pollution* 2017; 223: 575-586.

1014 Sulong NA, Latif MT, Khan MF, Amil N, Ashfold MJ, Wahab MIA, et al. Source  
1015 apportionment and health risk assessment among specific age groups during haze and non-haze  
1016 episodes in Kuala Lumpur, Malaysia. *Science of The Total Environment* 2017; 601-602: 556-  
1017 570.

1018 Sun Y, Chen C, Zhang Y, Xu W, Zhou L, Cheng X, et al. Rapid formation and evolution of an  
1019 extreme haze episode in Northern China during winter 2015. *Scientific Reports* 2016a; 6.

1020 Sun Y, Guan Z, Hooman K. A review on the performance evaluation of natural draft dry cooling  
1021 towers and possible improvements via inlet air spray cooling. *Renewable and Sustainable*  
1022 *Energy Reviews* 2017; 79: 618-637.

1023 Sun Y, Wang Z, Wild O, Xu W, Chen C, Fu P, et al. “APEC Blue”: Secondary Aerosol  
1024 Reductions from Emission Controls in Beijing. *Scientific Reports* 2016b; 6: 20668.

1025 Tan D, Zhou X, Xu Y, Wu C, Li Y. Environmental, health and economic benefits of using  
1026 urban updraft tower to govern urban air pollution. *Renewable and Sustainable Energy Reviews*  
1027 2017; 77: 1300-1308.

1028 Tang M, Chen S-C, Chang D-Q, Xie X, Sun J, Pui DYH. Filtration efficiency and loading  
1029 characteristics of PM2.5 through composite filter media consisting of commercial HVAC  
1030 electret media and nanofiber layer. *Separation and Purification Technology* 2018; 198: 137-  
1031 145.

1032 Tu R, Hwang Y. Reviews of atmospheric water harvesting technologies. *Energy* 2020; 201:  
1033 117630.

1034 VanReken TM, Nenes A. Cloud Formation in the Plumes of Solar Chimney Power Generation  
1035 Facilities: A Modeling Study. *Journal of Solar Energy Engineering* 2009; 131.

1036 Wang X, Zhang L, Moran MD. Uncertainty assessment of current size-resolved  
1037 parameterizations for below-cloud particle scavenging by rain. *Atmospheric Chemistry and*  
1038 *Physics* 2010; 10: 5685-5705.

1039 Wei H, Huang X, Chen L, Yang L, Du X. Performance prediction and cost-effectiveness  
1040 analysis of a novel natural draft hybrid cooling system for power plants. *Applied Energy* 2020;  
1041 262.

1042 Wu D, Xueyan B, Deng X, Li F, Tan H, Guolian L, et al. Effect of atmospheric haze on the  
1043 deterioration of visibility over the Pearl River Delta. *Acta Meteorologica Sinica* 2007; 21.  
1044 Wu Y, Ming T, de Richter R, Höffer R, Niemann H-J. Large-scale freshwater generation from  
1045 the humid air using the modified solar chimney. *Renewable Energy* 2020; 146: 1325-1336.  
1046 Xu Y, Zhou X, Cheng Q. Performance of a large-scale solar updraft power plant in a moist  
1047 climate. *International Journal of Heat and Mass Transfer* 2015; 91: 619-629.  
1048 Y.H.Pui D, Chen S-C, Zuo Z. PM<sub>2.5</sub> in China: Measurements sources visibility and health  
1049 effects and mitigation. *Particuology* 2014; 13: 1-26.  
1050 Yoo J-M, Lee Y-R, Kim D, Jeong M-J, Stockwell WR, Kundu PK, et al. New indices for wet  
1051 scavenging of air pollutants (O<sub>3</sub>, CO, NO<sub>2</sub>, SO<sub>2</sub>, and PM<sub>10</sub>) by summertime rain. *Atmospheric*  
1052 *Environment* 2014; 82: 226-237.  
1053 Yu S. Water spray geoengineering to clean air pollution for mitigating haze in China's cities.  
1054 *Environmental Chemistry Letters* 2014; 12: 109-116.  
1055 Yu S. Fog geoengineering to abate local ozone pollution at ground level by enhancing air  
1056 moisture. *Environmental Chemistry Letters* 2019; 17: 565-580.  
1057 Yu S, Li P, Wang L, Wang P, Wang S, Chang S, et al. Anthropogenic aerosols are a potential  
1058 cause for migration of the summer monsoon rain belt in China. *Proceedings of the National*  
1059 *Academy of Sciences* 2016; 113: E2209.  
1060 Zanoletti A, Bilo F, Depero LE, Zappa D, Bontempi E. The first sustainable material designed  
1061 for air particulate matter capture: An introduction to Azure Chemistry. *Journal of*  
1062 *Environmental Management* 2018; 218: 355-362.  
1063 Zhao Y, Sun F, Long G, Huang X, Huang W, Lyv D. Comparative study on the cooling  
1064 characteristics of high level water collecting natural draft wet cooling tower and the usual  
1065 cooling tower. *Energy Conversion and Management* 2016; 116: 150-164.  
1066 Zheng Y, Che H, Xia X, Wang Y, Wang H, Wu Y, et al. Five-year observation of aerosol  
1067 optical properties and its radiative effects to planetary boundary layer during air pollution  
1068 episodes in North China: Intercomparison of a plain site and a mountainous site in Beijing.  
1069 *Science of The Total Environment* 2019; 674.  
1070 Zhong J, Zhang X, Wang Y. Reflections on the threshold for PM<sub>2.5</sub> explosive growth in the  
1071 cumulative stage of winter heavy aerosol pollution episodes (HPEs) in Beijing. *Tellus B:*  
1072 *Chemical and Physical Meteorology* 2019a; 71: 1-7.  
1073 Zhong J, Zhang X, Wang Y, Liu C, Dong Y. Heavy aerosol pollution episodes in winter Beijing  
1074 enhanced by radiative cooling effects of aerosols. *Atmospheric Research* 2018; 209: 59-64.  
1075 Zhong J, Zhang X, Wang Y, Sun J, Zhang Y, Wang J, et al. Relative contributions of boundary-  
1076 layer meteorological factors to the explosive growth of PM<sub>2.5</sub> during the red-alert heavy  
1077 pollution episodes in Beijing in December 2016. *Journal of Meteorological Research* 2017; 31:  
1078 809-819.  
1079 Zhong J, Zhang X, Wang Y, Wang J, Shen X, Zhang H, et al. The two-way feedback  
1080 mechanism between unfavorable meteorological conditions and cumulative aerosol pollution  
1081 in various haze regions of China. *Atmospheric Chemistry and Physics* 2019b; 19: 3287-3306.  
1082 Zhou X, Wang F, Ochieng RM. A review of solar chimney power technology. *Renewable and*  
1083 *Sustainable Energy Reviews* 2010; 14: 2315-2338.

1084 Zhou X, Xu Y. Solar updraft tower power generation. *Solar Energy* 2016; 128: 95-125.

1085 Zhou X, Xu Y, Yuan S, Wu C, Zhang H. Performance and potential of solar updraft tower used  
1086 as an effective measure to alleviate Chinese urban haze problem. *Renewable and Sustainable*  
1087 *Energy Reviews* 2015; 51: 1499-1508.

1088 Zhou X, Yang J. A Novel Solar Thermal Power Plant with Floating Chimney Stiffened onto a  
1089 Mountainside and Potential of the Power Generation in China's Deserts. *Heat Transfer*  
1090 *Engineering* 2009; 30: 400-407.

1091 Zhou X, Yang J, Ochieng RM, Li X, Xiao B. Numerical investigation of a plume from a power  
1092 generating solar chimney in an atmospheric cross flow. *Atmospheric Research* 2009a; 91: 26-  
1093 35.

1094 Zhou X, Yang J, Wang F, Xiao B. Economic analysis of power generation from floating solar  
1095 chimney power plant. *Renewable and Sustainable Energy Reviews* 2009b; 13: 736-749.

1096 Zhou X, Yang J, Xiao B, Shi X. Special Climate around a Commercial Solar Chimney Power  
1097 Plant. *Journal of Energy Engineering* 2008; 134: 6-14.

1098 Zhu X, Wang Y, Zou Z, Gong H, Liu Z, Yan W. Investigation of the crosswind effect on the  
1099 performance of the atmospheric air purification tower. *The Journal of Engineering* 2019; 2019:  
1100 310-313.

1101 Zhu Z, Zhang M, Huang Y, Zhu B, Han G, Zhang T, et al. Characteristics of the planetary  
1102 boundary layer above Wuhan, China based on CALIPSO. *Atmospheric Research* 2018; 214:  
1103 204-212.

1104 Zou Z, Gong H, Lie X, Li X, Yang Y. Numerical investigation of the crosswind effects on the  
1105 performance of a hybrid cooling-tower-solar-chimney system. *Applied Thermal Engineering*  
1106 2017; 126: 661-669.

1107 Zuo L, Qu N, Ding L, Dai P, Liu Z, Xu B, et al. A vortex-type solar updraft power-desalination  
1108 integrated system. *Energy Conversion and Management* 2020; 222: 113216.

1109